ABSTRACT

Title of dissertation: RNA PACKAGING AND GENE DELIVERY USING TMV PSEUDO VIRIONS

Chi-Wei Hung, Doctor of Philosophy, 2008

Dissertation directed by Professor William E. Bentley
Fischell Department of Bioengineering

RNA interference (RNAi) has emerged as a powerful tool for the study of gene function and post-transcriptional regulation. However, the lack of a proper delivery system for RNAi is a major problem for its application as a therapeutic agent. In this study, *Tobacco mosaic virus* (TMV) is utilized as an RNAi carrier for gene delivery into mammalian and insect cells. The self assembly and disassembly of TMV is investigated to create chimeric viruses for gene delivery. The origin of assembly sequence (OAS) within the TMV RNA initiates its association with coat protein through a unique hairpin structure. Studies in this dissertation show that by incorporating TMV OAS into an RNA of interest, the RNA can assemble into “pseudo-virions” by the virus coat protein. The length of the pseudo-virions changed in proportion with the size of the RNA. To deliver the

RNA to the targeted cells, virions are further surface-modified with synthetic cell-penetrating peptides to facilitate cell endocytosis.

Two genes were selected as targets: 1) EGFP as a visual marker and 2) Cyclin E for control of cell cycle. EGFP is expressed in a transient expression experiment using a plasmid vector, pEFGP-N1. Cyclin E is regulated endogenously in High Five™ cells, and its translation is targeted using the pseudo virions. Pseudo-virions targeting *EGFP* RNA (antisense *EGFP*) are able to suppress transient EGFP production by 61% whereas pseudo virions targeting cyclin E (antisense *cycE*) are capable of arresting cells at G1 phase. This RNA packaging system protects packaged RNA and provides a means of delivering RNAi constructs into various host cells.

RNA PACKAGING AND GENE DELIVERY USING *TOBACCO MOSAIC VIRUS* PSEUDO VIRIONS

by

Chi-Wei Hung

Dissertation submitted to the Faculty of the Graduate School of the
University of Maryland, College Park in partial fulfillment
of the requirements for the degree of
Doctor of Philosophy
2008

Advisor Committee:

Professor William E. Bentley, Chair
Professor James N. Culver
Professor Sheryl H. Ehrman
Professor Peter Kofinas
Professor Nam S. Wang
Professor William A. Weigand

Dedication

To my parents Long-Ying Cheng and Sy-Wen Horng

Acknowledgements

I would like to acknowledge my advisors, Drs. William E. Bentley and James Culver, for their support, guidance, encouragement, and friendship during my studies here at the University of Maryland, College Park.

I would like to thank my dear lab mates in Bentley's and Culver's Lab. Hsuan-Chen Wu, Andrew Zayac and Dr. Chen-Yu Tsao helped me conduct cell cycle experiments. DT Howarth, a talented junior, provided great helps in RNA synthesis. I also appreciate the assistance from Rohan Fernandes, Colin Hebert, Karen Carter, Adam Brown, Drs. Sara Hooshangi, Liz Royston, and Sabrina Kramer, who helped me with the correction of this dissertation.

I am grateful to Amy Beaven for her help with the confocal microscopy, and Tim Maugel and Larry Lai for electron microscopy. Without their help, this project would not been possible.

This research was funded by United States Department of Agriculture (NR1-05-35-603-16278).

Table of Contents

LIST OF FIGURES

LIST OF TABLES

1 INTRODUCTION

1.1 Motivation

RNA interference (RNAi), also known as gene silencing, describes any RNA molecule (usually 21-25 nt) that interferes with expression of its corresponding gene product. RNAi has emerged as a powerful tool for characterizing the functions of specific gene expression and post-transcriptional regulation in eukaryotic organisms. The major advantages of using RNAi in gene silencing include its specificity of gene targeting and minimal long-term effects on the host cell. While RNAi has been a tremendous resource for studying genotype-phenotype relationships without the laborious use of gene knockout techniques, it has also been suggested to apply this technique for therapeutic purposes. However, the major bottleneck in the development of RNAi therapy is the delivery of the macromolecules to the cell, organ, or tissue. Under physiological conditions, siRNAs (small interfering RNAs, 21-mer) will not readily cross the cellular membrane due to their charge and size. Consequently, a reliable RNAi delivery approach is of special interest and has become a key issue in developing gene therapy using RNA gene silencing.

In search of a delivery system for RNAi gene silencing, current gene delivery protocols are under review. Cellular delivery of *in vitro* synthesized siRNAs across the membrane can be achieved by cationic-liposome-based strategy – the most popular method for transfection. The drawback of using cationic liposomes *in vivo* is the rapid liver clearance of the liposome and the lack of targeted organ specificity (Sioud and Sorensen 2003; Sorensen, Leirdal et al. 2003). Therefore, an effective delivery system

should be able to preserve the genetic material until entering the cell and a better cell targeting strategy is desirable. This is particularly a challenge for RNA delivery due to the natural instability of RNA. From this point of view, viral vectors for RNA delivery have shown their strong advantages in providing protection to their genetic materials. Viral vectors for gene delivery, such as adenovirus (e.g. flu) (Lin, Chen et al. 2006), retrovirus (e.g. HIV) (Jia, Zhang et al. 2006), and herpes simplex virus (e.g. chickenpox) (Saydam, Glauser et al. 2005) can also generally achieve high transfection rates. However, viral vectors may induce immune responses and have been reported to integrate their genomes into the host (Schagen, Rademaker et al. 2000). On the other hand, while gene delivery systems, such as non-viral plasmids and the aforementioned cationic lipids, are easily available and suitable for a large variety of cells, these systems typically result in low transfection yields.

We investigate the idea of using a plant virus as a gene carrier, instead of a human viral vector, to minimize the risk of viral mutation post-infection. *Tobacco mosaic virus* (TMV) provides an ideal model for RNAi gene delivery because of its simple virion structure and well-characterized genome. Viruses are naturally occurring gene vehicles that protect genetic material until its release for propagation upon delivery to a specific host. In order to utilize TMV as a RNA vehicle for gene delivery, three major challenges need to be addressed in this research: 1) Designing a protocol for creating the recombinant RNA of interest which can be either transcribed *in vivo* or synthesized *in vitro*, 2) Encapsulating the targeted RNA in the TMV virion, and 3) Developing a delivery strategy for a plant virus endocytosis targeting mammalian cells.

To explore the first of the three considerations, the RNA of interest can either be transcribed *in vivo* by a viral vector in the host, or synthesized *in vitro* followed by gene delivery. In both cases, DNA recombination will be needed to incorporate the RNA of interest into viral vectors or plasmids for RNA synthesis. In this study, the latter method is chosen in order to reduce the risk of pathogenicity or the possibility of gene integration into the host genome. Particularly, after RNA synthesis *in vitro*, TMV virions will be utilized as a gene vehicle to carry RNA cargo, rather than as an infectious viral vector. An infectious viral vector usually inserts the gene of interest into the host genome so that the gene of interest is transcribed by the host genetic machinery. As a gene delivery vehicle, the TMV virion here does not replicate in the host.

The second challenge of this work is to demonstrate the encapsulation of the RNA by the TMV coat protein. The encapsulation can occur by mixing TMV coat protein with the synthesized RNA at certain physiological conditions. In a previous study, the mechanisms of TMV virion disassembly and re-assembly were characterized and performed *in vitro* (Fraenkel-Conrat and Williams 1955). In this research, this viral assembly system will be utilized as an RNA vehicle for targeted gene delivery.

The last challenge of the TMV pseudo-virions is the delivery of the assembled system to host cells and the release the RNAi for gene silencing. For a plant virus to be able to cross the mammalian cell membrane, surface modification on the TMV virion may enable cell targeting and facilitate virion endocytosis. This research will explore the methods of crosslinking modification of TMV surface, as well as in the endocytotic pathway.

The work proposed here will address RNAi delivery using the TMV virion where the RNAs of interest will be cyclin E and green fluorescent protein (GFP). The project scope, the hypothesis, and the proposed approach will be discussed after the literature review.

1.2 Tobacco mosaic virus

1.2.1 Early milestone in the research on *Tobacco mosaic virus*

Tobacco mosaic virus has played a leading role in the development of virology for more than a century. The first dated report came in 1886 when Adolf Mayer described the retardation of growth, decreased yield, and the accompanying curling and brittleness of leaves that makes the tobacco leaves unwelcome for cigar making. It was Mayor who named the syndrome "tobacco mosaic" due to the pattern of light and dark green on the foliage. His most influential discovery was, however, that the condition was infectious and could be induced by the juice from diseased leaves. He looked for pathogens but failed to find any, although he noted that the infectivity disappeared by prolonged heating at 80^{o}C (Reviewed by (Harrison and Wilson 1999)).

Ivanowski studied the tobacco mosaic disease and published his paper in 1892 (Ivanowski 1892) where he claimed that the extracts of the mosaic-affected leaves remain infective after passing through filters designed to be impassable to bacteria. Martinus W. Beijerinck in 1898 repeated the filtration experiments and concluded that it propagated in the plant but not *in vitro*. The multiplication occurred best in actively growing cells. He reported the disease agent to be either soluble or too small to be filtered out by bacteria filters, and named it *contagium vivum fluidum* ('soluble living germ'). This description was the first recognition of a new category of infectious agents we now call viruses (Harrison and Wilson 1999).

1.2.2 Structure/Morphology analysis of TMV virion

After more than a century of studies, we have a better understanding of the TMV crystal structure and the two key components – coat proteins and viral RNA. TMV (U1 strain) virion is rod-like (18nm x 300nm) and composed of 2,130 identical coat protein (CP) units stacked in a helix around a single strand of plus sense RNA of 6,395 nucleotides (nt)(Reviewed by (Okada 1986; Stubbs 1990)). TMV CP (17.5 kD) can form three general classes of aggregates – the 4S or A protein consisting of a mixture of low-order aggregates (monomer, dimer, trimer), the 20S disc or helix composed of 38 subunits, and an extended virion-like rod (Fig 1-1). Ionic strength, temperature, and pH in the cytoplasm determine the electrostatic properties on the coat protein surface and lead to protein association and disassociation (Durham, Finch et al. 1971).

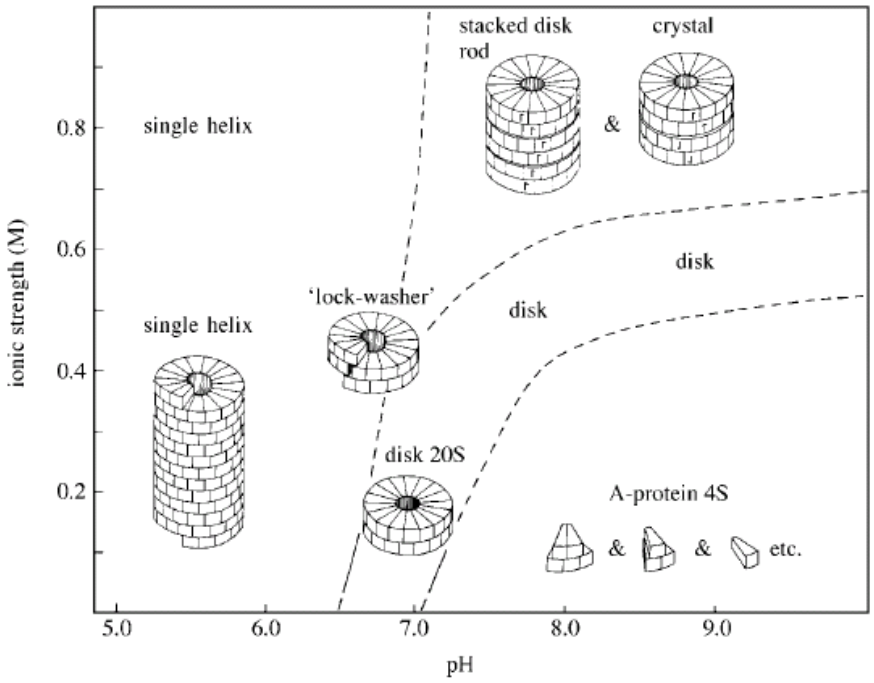

Figure 1-1 Diagram showing the ranges over which particular species of TMV coat protein anticipate extensively in equilibrium. Without RNA present, long helical structure prevails on TMV morphology at pH 5. At low ionic strength and pH > 7.5, the majority of CP form small "A-protein" aggregates. However, the 20S disc-protein is abundant only at a narrow window of pH ~7.0, which is critical for virion assembly (Durham, Finch et al. 1971).

In 1955 Fraekel-Conrat demonstrated that an infectious TMV virion could be reconstructed *in vitro* from its protein subunits and RNA (Fraenkel-Conrat and Williams 1955). The *in vitro* formed virus particles were indistinguishable from its native form of virus in terms of biological and physicochemical properties. This study will utilize the ability of TMV to self-assembly as an RNA carrier for gene delivery.

1.2.3 TMV virion and its assembly

The 20S protein disc (as shown in Fig. 1-1) plays a crucial role in the assembly of the virus from its RNA and protein. The disc interacts with a specific initiation tract on the single strand viral RNA, called the "origin of assembly sequence" or OAS, to begin the helix growth. TMV OAS is a purine-rich stem loop structure located 872-958nt from the 3' end of the TMV RNA (Jonard, Richards et al. 1977; Zimmern and Butler 1977; Okada, Fukuda et al. 1980). In various TMV strains, a sequence, 5'-AAGARGUUG-3', is commonly found in the loop of OAS (where R=A or G). The association of the RNA with CP is predicted to be initiated by insertion of the OAS stem-loop into the central hole of the 20S disc aggregates and between the two layers of subunits (Fig. 1-2) (Butler, Bloomer et al. 1976; Turner, Joyce et al. 1988; Gaddipati and Siegel 1990). RNA without the OAS will be rejected for viral assembly. Based on the X-ray studies of the CP disc, the adjacent two layers of the discs are arranged so as to leave a gap in between them, effectively acting like a 'jaw' to 'hold' the RNA prior to initiating viral assembly (Bloomer, Bricogne et al. 1978; Bloomer, Champness et al. 1978). Right after insertion, the loop of RNA OAS binds around the first turn of the 20S disc, opening up the base-paired stem as it does so. This causes a conformational change in the disc permitting the formation of short stable helical nucleus for rod elongation. Once the assembly initiates,

no specific RNA sequences are necessary for conducive elongation since the interaction between the negatively charged RNA and positive charged peptides seems to be sufficient for the conformational change of the protein subunit in the 20S disc (Meshi, Ohno et al. 1981; Turner and Butler 1986; Gaddipati and Siegel 1990).

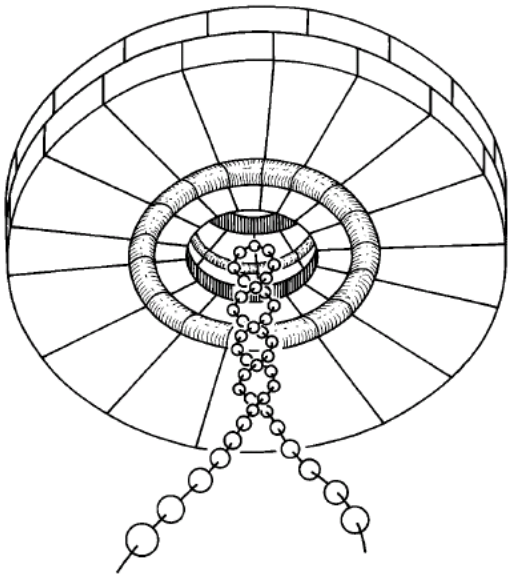

Figure 1-2 Initiation of the virus assembly. Nucleation of the TMV begins with the insertion of the hairpin loop formed by the OAS into the central hole of the protein disc. (Butler, Bloomer et al. 1976; Klug 1999)

1.2.4 TMV disassembly: *in vivo* and *in vitro*

The paradox of the TMV virion is that it must remain stable in the extracellular environment, but upon cell entry it must destabilize and disassemble in order to release the RNA for viral translation. The switch between stability and instability requires a molecular mechanism capable of sensing subtle changes in the environment. In fact, the TMV virion is an extremely stable structure, having been reported to retain infectivity in non-sterile extracts at room temperature for at least 50 years (Silber and Burk 1965). The stability of virus and infectivity is a consequence of interactions between coat protein subunits, as well as, between coat protein and RNA.

Structure studies of TMV have identified a switching mechanism provided by the intersubunit clusters of carboxyl-carboxylate groups from glutamic acid (E) or aspartic acid (D) located at the interface between adjacent CP subunits. Under stabilizing conditions, the repulsive interactions made by the negatively charged carboxylate groups are stabilized by the presence of positively charged calcium ions (Ca^{2+}) or protons (H^{+}) (Durham, Hendry et al. 1977; Durham 1978). When a virion enters a plant cell, the high pH (low proton) and low calcium environment in the cell (compared to extracellular conditions) leads to the loss of stabilizing ions, allowing the repulsive negatively charged carboxylate groups to interact, which leads to virion destabilization (Caspar 1963; Namba, Pattanayek et al. 1989). Particularly for TMV, the repulsive force has the greatest effect at the 5' end of the RNA. This is because CP-RNA interactions are strongest for guanine (G) and no guanine residues are present in the first 69 nt of the 5' end RNA (Goelet, Lomonossoff et al. 1982; Steckert and Schuster 1982). The absence of G residues enables the CP protein subunit at the 5' terminus to be preferentially dislodged (Mundry,

Watkins et al. 1991), making the 5' end of the virion the "weak point" in the viral structure for disassembly.

Based on available structural information, steps involved in TMV virion disassembly *in vivo* can be envisioned as follows. First, mechanical damage to the cell wall and plasma membrane allows virion entry into the cytoplasm. The high pH and low calcium environment in the plant cell destabilizes the CP subunits to expose the 5' end of RNA. The ribosomes then bind to the exposed RNA and initiate the translation of the replicase ORF (Gallie, Sleat et al. 1987; Sleat, Gallie et al. 1987; Gallie, Sleat et al. 1988). The active translation provides the energy needed to disassemble the CP subunit and subsequently strip the RNA further downstream toward the 3' end (Wilson 1984; Shaw, Plaskitt et al. 1986; Wilson and Shaw 1986).

TMV virion disassembly can be conducted *in vitro* by various treatments: glacial acetic acid (Fraenkel-Conrat 1957), hydrochloric acid (Choi, Park et al. 2000), urea (Buzzell 1960; Drygin, Bordunova et al. 1998), mild alkaline (Durham 1972; Drygin, Bordunova et al. 1998), SDS (Kado and Knight 1966; Wilson, Perham et al. 1976), and dimethyl sulfoxide (DMSO) (Nicolaie, Lebeurie et al. 1974; Drygin, Bordunova et al. 1998). In this study, glacial acetic acid was selected for TMV stripping to remove viral RNA and to collect CP without disrupting its reassembly capabilities. TMV viral RNA, once exposed to acetic acid, precipitates and can easily be removed by centrifugation. The RNA-free TMV CP can be recovered by a de-salting column or dialysis for further analysis.

1.2.5 TMV genome

At the nucleotide level, both translated and untranslated TMV genome sequences possess several significant properties for viral protein expression and virion structure (Fig. 1-3). The 5' leader sequence of the TMV RNA untranslational region (5'-UTR) effectively acts as a ribosomal binding site (RBS) (Tyc, Konarska et al. 1984) and a translational enhancer both *in vitro* and *in vivo* (Gallie, Sleat et al. 1987; Gallie, Sleat et al. 1988). The 3' untranslational region (3'-UTR) can enhance *in vitro* protein translation more than 3-fold(Zeyenko, Ryabova et al. 1994). Additionally, the aforementioned OAS, located around 1,000 nt from the 3' termini, is essential to virion assembly due to its unique stem-loop structure.

As for the viral proteins encoded by TMV genome, the single strand positive sense RNA has been sequenced (Goelet, Lomonossoff et al. 1982) and 4 open reading frames (ORFs) have been found and studied: the 126-kDa and 183-kDa proteins of replicase, the 30-kDa movement protein, and the aforementioned 17.5-kDa coat protein. The 5'-most ORF of TMV genome encodes a 126-kDa RNA replicase which also contains a motif characteristic of methyl transferase and helicase domain (Lewandowski and Dawson 2000). Readthrough of the amber terminator (UAG) to the next ORF of 54 kDa RNA dependent RNA polymerase (RdRP) yields a 183 kDa RNAP (Pelham 1978; Lewandowski and Dawson 2000) while the 54-kDa RdRP itself has not been detected *in vivo*(Canto, MacFarlane et al. 2004). The 30-kDa movement protein is believed to facilitate virus movement based on the inability of TMV to cause a systemic spread of infection upon deletion of the movement protein ORF (TMVΔMP) (Arce-Johnson, Reimann-Philipp et al. 1997). The 3'-most ORF encodes a 17.5 kDa protein known as the TMV CP. However, only the 126 kDa and 183 kDa replicase protein are required for

replication of the genomic RNA or various defective RNAs generated *in vitro* (Lewandowski and Dawson 2000). Lastly, only the 126 kDa protein, not its RNA, has been shown to suppress gene silencing (Ding, Liu et al. 2004).

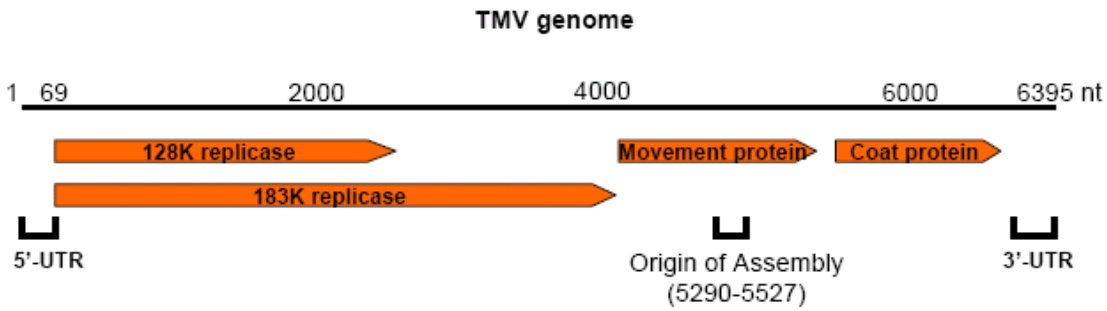

Figure 1-3 TMV genome. Wild-type TMV (U1 strain) contains 6395 nt, encoding 4 ORFs: 126 kDa and 183 kDa replicase, 30 kDa movement protein (MP), and 17.5 kDa coat protein (CP). Solid line represents the viral RNA (1-6395), while 4 orange boxes indicate ORFs and their relative positions on the TMV genome. 183-kDa replicase is translated as a readthrough of the terminating codon at the end of 126-kDa replicase.

In this study of RNA interferences using TMV virion, the recombinant RNA was constructed by replacing the majority of the 126-kDa ORF with specific genes of interest, such as cyclin E and GFP. The resulting RNA would retain the 5'-UTR, the 3'UTR, and the OAS so that viral assembly can take place. Importantly, the 126-kDa replicase RNA has been selectively deleted in order to disrupt its viral infectivity to plants, and to minimize the possibility of suppressing the RNA interference activities. The recombinant RNA construction is illustrated in Chapter 3.

1.3 RNA interference

The specific mRNA depletion in *Caenorhabditis elegans* by double stranded RNA (dsRNA) drew broad interest and formed the basis for the discovery of RNA interference (RNAi) (Fire, Xu et al. 1998). The striking finding was that dsRNA injected into the animals had twice the interfering potency than either strand individually. However, the phenomenon of dsRNA induced gene silencing in plants had been known for some years before the *C. elegans* experiments were revealed (review in (Matzke 2002)). The core concept of RNAi is the processing of dsRNA into small interfering RNA (siRNA) segments of 21-25 nucleotides (nt) in length, the formation of a protein-siRNA complex, the binding of this complex to the mRNA, and finally, the degradation of the targeted mRNA. The following section will illustrate the mechanism in detail.

1.3.1 Mechanism of dsRNA as RNAi

Since the RNAi activity was found in C. elegans (Fire, Xu et al. 1998), scientists have observed the depletion of mRNA in many other host cells: *Drosophila melanogaster* (Clemens, Worby et al. 2000), High Five (insect) (Beck and Strand 2003), *Arabidopsis thaliana* (plant) (Chuang and Meyerowitz 2000), *Neurospora crassa* (fungi), mouse embryonic stem cells (Wianny and Zernicka-Goetz 2000; Yang, Tutton et al. 2001), HEK293 (Elbashir, Harborth et al. 2001; Morimoto, Okamura et al. 2004) and HeLa cells (Elbashir, Harborth et al. 2001). Studies using Drosophila embryo lysates and cultured S2 cells support a four-step model for the mechanism of RNAi.

The model proposes that RNAi is intiated by the ATP-dependent, progressive cleavage of long dsRNA into 21-25nt double-stranded fragments, termed small

interefering RNAs (siRNAs). These siRNA duplexes are incorporated into a protein complex (protein-siRNA complex) that is not yet competent to mediate RNAi. Instead, ATP-dependent unwinding of the siRNA duplex remodels the complex to produce an active RNA-induced silencing complex (RISC). Finally, in a step that requires little or no ATP, the RISC can recognize and cleave a target RNA complementary to the guide strand of the siRNA.

Specifically, siRNAs are produced by the enzyme Dicer, a member of the RNase III family. Dicer can chop dsRNA into two classes of smaller RNAs – miRNAs (microRNAs) and siRNAs. Although chemically similar to siRNAs (Zeng, Yi et al. 2003), miRNAs are formed by Dicer cleavage of hairpin-loop RNA precursors rather than long double-stranded RNAs. (Nakahara and Carthew 2004; Tang 2005) These miRNA precursors are transcribed from endogenous genes within the genome, whereas siRNAs are usually originated from exogenous species (e.g. virus and transgenes) (Carthew 2001; Hannon 2002; Meister and Tuschl 2004) (Fig. 1-4).

1.3.2 MicroRNAs originate from endogenous dsRNA hairpins

Found in many eukaryotic cells, miRNAs originate from genome where endogenous transcripts (called primary miRNA transcripts) that contain 20-50 base pair complementary inverted repeats fold back on themselves to form dsRNA hairpins (Fig. 1-4). In the nucleus, this dsRNA hairpin is processed by an RNase endonuclease, Drosha, to form the miRNA precursor, which can be exported to the cytoplasm by the nuclear export receptor, exportin-5. Once in the cytoplasm, this miRNA precursor, following a pathway similar to siRNA, is cleaved by Dicer to yield an RNA duplex of 21-25 nt in length.

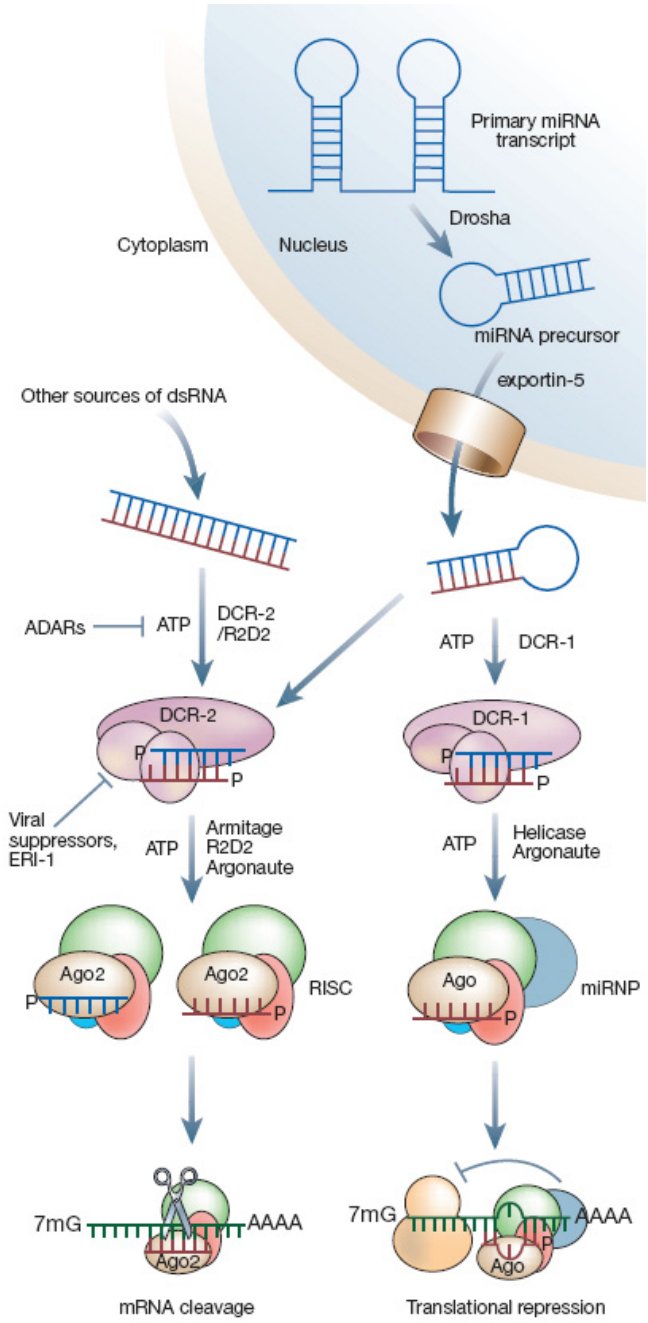

Figure 1-4 Model of RNAi gene regulation: miRNA (right) and siRNA (left)
In the nucleus, primary miRNA transcripts (pri-miRNA) are processed to miRNA precursors (pre-miRNA) by the RNase-III-like enzyme Drosha. The pre-miRNA is exported to the cytoplasm by the export receptor exportin-5. The pre-miRNA is further processed by Dicer to siRNA-duplex-like intermediates. The duplex is unwound while assembling into miRNP/RISC. Mature miRNAs bind to Argonaute (Ago) proteins, which mediate translational repression and/or cleavage of target mRNAs. Like pre-miRNA, long dsRNA is processed by the RNase III enzyme Dicer into 21–25 nucleotide dsRNA intermediates. Assisted by the RNA helicase Armitage and R2D2, the single-stranded siRNA-containing RISC is formed. (Meister and Tuschl 2004)

Dicer delivers the siRNAs (or miRNAs) to a group of proteins called RISC (RNA-Inducing Silencing Complex) that use the antisense strand of the siRNA to bind to and degrade the corresponding mRNA, resulting in gene silencing (Fig. 1-5). Similar to other products from RNAse III endonucleases, siRNA duplexes contain a 5' phosphate and a 3' hydroxyl termini, and two single-stranded nucleotides on their 3' end, all essential to the RNAi pathway. It has been found that blunt-ended siRNAs or siRNAs lacking a 5' phosphate terminus are inefficient in triggering RNAi, both *in vivo* and *in vitro* (Nykanen, Haley et al. 2001).

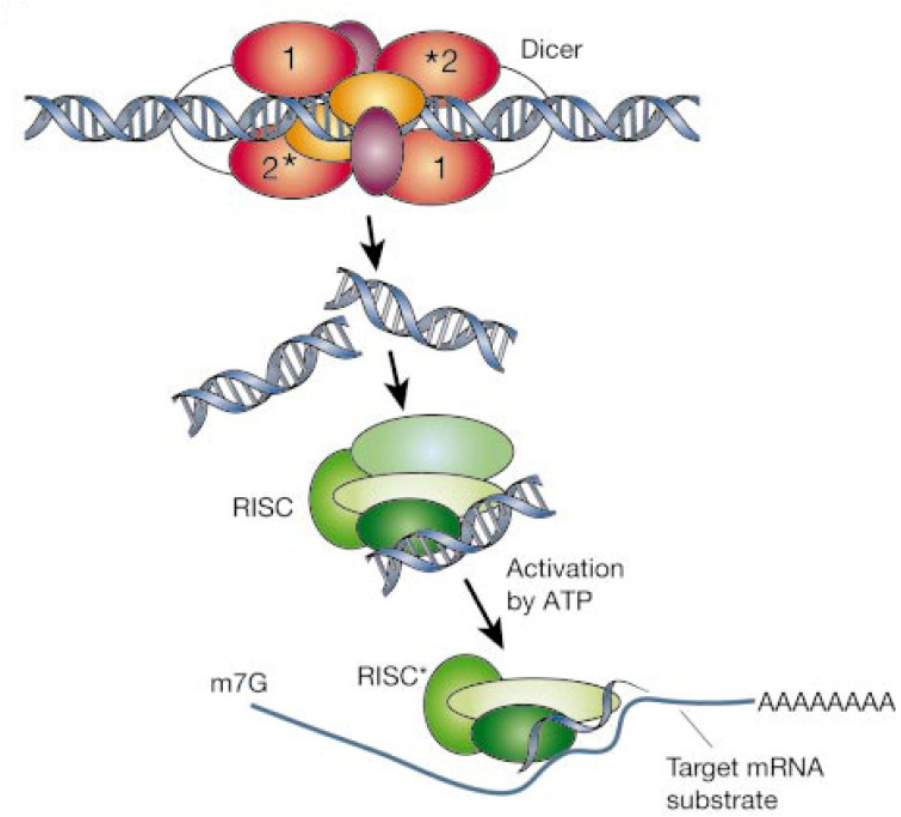

Figure 1-5 Dicer and RISC for gene silencing. RNAi is initiated by the Dicer enzyme which processes dsRNA into ~21-25 nucleotide siRNAs. The siRNAs are incorporated into a multicomponent nuclease, RISC (green). Recent reports suggest that RISC must be activated from a latent form, containing a double-stranded siRNA, to an active form (RISC*) by unwinding siRNAs. RISC* then uses the unwound siRNA as a guide to substrate selection. Figure adapted from (Hannon 2002)

1.3.3 Single strand siRNA vs. double strand siRNA

The first siRNA study by Fire et al in 1998 showed that dsRNAs were more effective in producing interference than either sense strand or antisense strand individually(Fire, Xu et al. 1998). However, it is generally agreed that not only dsRNAs, but antisense ssRNAs and, surprisingly, the sense ssRNAs can all deplete corresponding mRNA via gene silencing (Guo and Kemphues 1995; Martinez, Patkaniowska et al. 2002; Schwarz, Hutvagner et al. 2002; Holen, Amarzguioui et al. 2003; Hall, Wan et al. 2006; Raemdonck, Remaut et al. 2006). Other observations from previous studies comparing antisense siRNA and double-stranded siRNA are summarized below:

1. Antisense siRNA reaches maximum activity faster than double strand siRNA. Standard double-stranded siRNA reaches maximum effect after ~24 hrs, after which the silencing fades away over 3-5 days. Antisense siRNA shows stronger mRNA depleting activities than double-stranded siRNA at 10 hr post-transfection. The maximum effect of antisense siRNA seems to be achieved at this time point as mRNA levels increased at later time points (Holen, Amarzguioui et al. 2003).
2. Since single-stranded antisense RNAs shows much less gene silencing ability than double stranded RNAs, dose-dependence experiments from two independent research teams demonstrated that double-stranded siRNAs were active at an ~4-6 fold lower concentration than antisense siRNA (Holen, Amarzguioui et al. 2003; Hall, Wan et al. 2006).
3. Intracellular degradation is more crucial to ssRNA than to dsRNA (Raemdonck, Remaut et al. 2006). Duplexed siRNA shows a more persistent result than

antisense siRNA in gene silencing, primarily attributed to their differences in susceptibility to nuclease attack (Bertrand, Pottier et al. 2002).

4. A study that targeted human tissue factor (hTF) mRNA in HaCaT cells suggested that antisense siRNA and double-stranded siRNA share a common RNAi pathway, due to 1) an almost identical target position effect, 2) an identical appearance of mRNA cleavage fragments, 3) a similar tolerance/intolerance for mutational and chemical backbone modifications, and 4) the fact that excess inactive double-stranded siRNA can competitively block antisense siRNA.(Holen, Amarzguioui et al. 2003)

1.4 Cyclins and cell cycles

1.4.1 Cell cycle in eukaryotic cells

Cell cycle is a series of events that takes place in a eukaryotic cell leading to its division. In 1953 Howard and Pelc first described cell cycle as four phases: G1, S, G2 and M (Fig 1-6A) (Dubrovsky and Ivanov 2003). The G1 and G2 phases of the cell cycle represents the two "gaps" that occur between the two more obvious landmarks: DNA synthesis (S phase) and mitosis (M phase). G1 is the gap between M phase and S phase when cells increase their mass and prepare for DNA synthesis. G2 is the gap between S and M phase when each cell carries two identical copies of chromosome DNA, waiting to divide into the two daughter cells in M phase. Non-proliferative cells enter quiescent state G0 (from G1) where cells does not expand or divide.

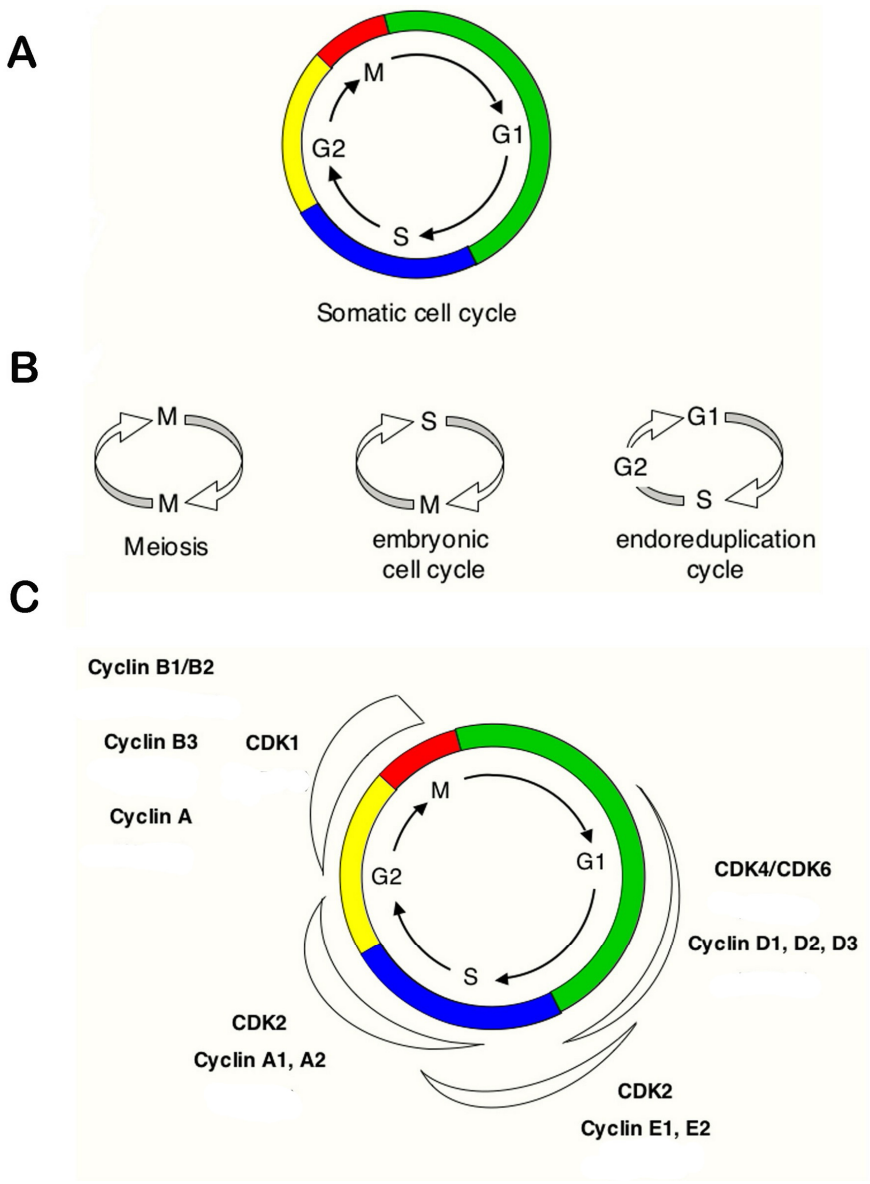

Figure 1-6 (A) Somatic cell cycle: M-G1-S-G2. (B) Variant of cell cycle in which specific phases are omitted. (C) Cell cycle control system. Arc shapes outside the cycle indicate the increase and reduction of the corresponding cyclin-CDK activity. For example, CDK2 and Cyclin E control the G1 to S checkepoint while CDK1 and cyclin B play essential roles in G2 to M transition (van den Heuvel 2005).

1.4.2 Variation of the cell cycle

Variations of the typical somatic division cycle shown in Fig 1-6 are found to fulfill specific requirements: rapid embryonic cells that lack G1 and G2 phases and meiotic cells that allow formation of haploid gametes (Fig. 1-6B). In addition, cell cycle regulation can be dramatically different from species to species, organ to organ, and even cell to cell. For example, in *Arabidopsis* root tips the cells on the meristem divide and expand (somatic cell cycle), whereas the cells on the same root in the elongation zone expand but do not divide (cell arrested in G1). The mature *Arabidopsis* root is the largest part of the root system, where the cell does not divide or grow (in G0) (Beemster, Fiorani et al. 2003).

1.4.3 Key molecules that control cell cycle regulation: cyclins, Cdks, and CKIs

Cell cycle involves numerous regulatory proteins that direct the cell through a specific sequence culminating in mitosis and the production of two daughter cells. Central to this process are cyclins, cyclin dependant kinases (Cdks, which complex with cyclins) and cdk inhibitors (CKI). In mammalian cells, nearly 20 cyclins and 10 cdks have been described, and each phase of the cell cycle has a unique profile of cyclin-cdk activity (Reviewed by Hwang (Hwang and Clurman 2005)). Although species-specific differences exist, the molecular details of cell cycle regulations are fairly conserved (Reviewed by Novak (Novak, Sible et al. 2003)). Oscillation in the activities of various cyclin-Cdk complexes leads to the initiation of various cell cycle events. For example, activation of the S-phase cyclin-Cdk complex initiates DNA replication, while the activation of M-phase cyclin-Cdk complex triggers mitosis (Fig. 1-6C). These protein

complexes and their inhibitors are essential to cell cycle regulation and function as "checkpoints" in the control of the cell cycle.

1.4.4 Checkpoints in the cell cycle

In most cells there are several checkpoints in the cell cycle, where the cycle can be arrested if the previous event is not complete. A cell cannot enter M phase when DNA replication is not complete (G2 checkpoint), and chromosome separation is delayed if some chromosomes are not properly attached to the mitotic spindle (Metaphase checkpoint).

Checkpoint mechanisms act through negative intracellular signals that arrest the cell cycle, rather than through the positive signals that normally stimulate cell cycle progression. A cell needs to monitor the attachment of all its chromosomes to the mitotic spindle prior to cell division. In other words, the cell needs to detect the last attachment of the chromosome to the microtubules of the spindle. In a cell, if each chromosome delivers a positive signal to cell cycle machinery once it attached, the last attachment would be hard to detect, as it is only a small fractional change on the signaling intensity. Instead, if each unattached chromosome sends a negative signal to the cell cycle machinery, the last negative signal will be easy to detect since it changes from negative to none (Alberts, Johnson et al. 2002). This negative control mechanism is commonly seen in biological pathways.

1.4.5 G1 checkpoint and G1–S phase cyclin dependent kinases (G1-S-Cdks)

The G1 checkpoint, in particular, is located at the end of the G1 phase, just before entry into S phase, allowing the cell to determine whether to divide, delay division, or

enter the resting phase (G0). This G1 checkpoint is mainly regulated by two types of cyclin-Cdk complexes: cyclin D, which binds to cdk4/6, and cyclin E, which activates cdk2. First, the negative signal molecule CKI, p16, which would normally inhibit cdk4/6 through an interaction with cyclin D1, is down-regulated, causing cell cycle progression to stop. In growth induced or oncogenic induced cyclin D expression (e.g. breast cancer), this checkpoint is overcome because increased expression of cyclin D allows its interaction with cdk4/6 by competing for binding(Sutherland and Musgrove 2002). Once active cdk4/6-cyclin D complexes form, the tumor suppressor retinoblastoma (Rb) phosphorylate to relieve the inhibition of the transcription factor E2F. E2F is then able to cause expression of cyclin E, which then interacts with CDK2 to allow G1 to S phase transition (Fig. 1-7).

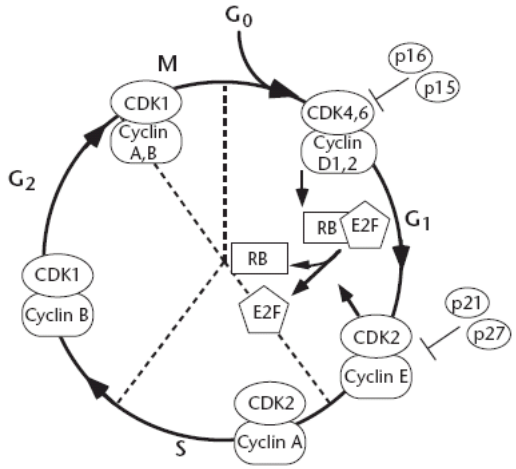

Figure 1-7 Simplified pathway of Cdks, CKIs, and cyclins. (Funk 2005)

1.4.6 Cyclin E : the key element for G1 checkpoint

Cyclin E-Cdk2 has long been considered an essential and master regulator of progression through G1. Cyclin E-Cdk2 activity is highest during G1-S phase (Fig. 1-7) and lowest in quiescent cells (G0) (Ekholm, Zickert et al. 2001). The periodical change of cyclin E-Cdk2 results from many factors including transcriptional and post-translational control of cyclin E, binding of Cdk inhibitors (e.g. p21 and p27, figure 1-7), and modification of Cdk2 activity by inhibiting and activating phosphorylations. These multiple mechanisms of cyclin E control will ensure cyclin E-Cdk2 acitivity to be tightly regulated during normal cell cycles. In cancer cells, however, cyclin E-Cdk2 is often deregulated and this is likely to contribute to the development of cancer. In fact, cyclin E is found to be over-expressed in several tumors including leukemia, carcinoma of the breast, colon, pancreas, and prostate (Clurman and Roberts 1995; Porter, Malone et al. 1997; Funk 2005). Moreover, cells were found to be arrested in G1 phase when cyclin E gene is knocked out or knocked down (Koff, Cross et al. 1991; Grassi, Schneider et al. 2005; March and Bentley 2007).

1.4.7 Flow cytometry, DNA content, and cell cycle

The analysis of cells stained with DNA-specific fluorochromes was one of the first applications of flow cytometry. This procedure can rapidly determine both DNA ploidy and cell cycle measurements. In G1 phase, the DNA content of each cell in an organism is highly uniform. When diploid (2N, N= number of gametes) cells are stained with a DNA targeting dye and analyzed by the flow cytometry, a narrow distribution of fluorescence intensities is obtained. This DNA content distribution is displayed as a

histogram of fluorescent intensity (x-axis) versus the number of cells with observed intensity. In S phase, cells begin DNA synthesis and the DNA content is greater than those in G1. As replication proceeds, the DNA content increases until the cell enters enter G2 phase with DNA content twice that of G1. Cells in G2 and M phase both possess tetraploid (4N) until cytokinesis occurs for cell division (Rabinovitch 1994).

Stoichiometry of DNA stains can be established from the ratio of the G2/M and G1 peak values in the DNA histograms. Ideally this ratio should be close to 2 since the cells in G2/M contain twice as much DNA content as those in G1 (4N:2N). Several methods have been proposed for DNA content analysis (Reviewed by Rabinovitch (Rabinovitch 1994)). One of the simplest graphic methods is based on the assumption that G1 and G2 phase fraction distribution are symmetric; therefore, each fraction can be approximated by examining the portion of the histogram where the G1 and G2 phases overlap with the S phase. The area under the left half of G1 curve is mirrored to the right half and the area under the right half of G2 curve is reflected to its left half. Those two symmetric bell shape curves are denoted as G1 and G2/M phases, and what remains is S phase. Other well established models include Dean and Jett (1974) and Fox (1980), both of which are based on the prediction of the theoretical cell cycle histogram as a result of Gaussian distribution and have been broadly applied in computer-based cell cycle analysis (Dean-Jett-Fox model)(Dean and Jett 1974; Fox 1980).

1.5 RNAi gene delivery for therapeutics and plant made virus for vaccine

In this section, current RNAi gene delivery methods are reviewed for a better understanding of the state-of-the-art technologies and their limitations. The applications of using plant virus as a vaccine are also presented in comparison to the viral delivery of RNAi.

1.5.1 RNAi gene delivery for therapeutics

Post-transcriptional gene silencing by RNA interference appears to be a promising new approach for the targeted inhibition of gene expression in cell culture and *in vivo*. The major advantages of RNA gene silencing are its specificity in gene targeting, controlled by the Watson-Crick base pair interactions (A-U, C-G), and the unrestricted choice of targets. The delivery of the siRNA, the key intermediate of RNAi, can elicit a potent knockdown of the desired protein for genotype-phenotype study without the arduous work needed for chromosomal gene knockouts. With the huge impacts on biological science in the past decade, there are currently several clinical trials, ongoing and planned, that utilize RNAi for the treatment of diseases such as macular degeneration, cancer, and respiratory diseases.

1.5.2 Clinical Trials using siRNA

The first human clinical trial using siRNA techniques was conducted in 2004 by Acuity Pharmaceuticals (which is merged and renamed as Opko) in patients suffering age-related macular degeneration (AMD). This treatment is now (as of June 2007) under Phase III clinical evaluation with preliminary results indicating a dose-dependent benefit being observed in terms of the decrease of lesions which characterize AMD(Akhtar and

Benter 2007; Liu, Wong-Staal et al. 2007). Sirna Therapeutics has entered their first clinical trials using siRNA targeting the vascular endothelial growth factor for the treatment of the same disease and is ongoing at Phase I. Alnylam Pharmaceuticals recently completed two Phase I trials on their RNAi treatment targeting *Respiratory syncytial virus* lung infection and pandemic flu (Akhtar and Benter 2007).

1.5.3 Challenges of RNAi gene therapy

Despite of the emergence of RNA interference in clinical trials, there are several hurdles to be overcome before gene silencing techniques can be used widely as therapeutics agents. Two of the major concerns are the instability of RNAi molecules and the lack of an efficient RNAi delivery to the target sites in the body. To enhance RNA stability, studies on RNA backbone modification have shown extended interfering activity *in vivo* (Hall, Wan et al. 2004; Hall, Wan et al. 2006). For the latter concern, a recent study published on *Nature* of April 3rd, 2008, drew much attention by indicating the positive results of siRNA therapeutic treatment of AMD (clinical trial conducted by Opko) was an outcome from a non-specific siRNA that triggered the immune response through toll-like receptor 3 (TLR-3) (Kalluri and Kanasaki 2008; Kleinman, Yamada et al. 2008). Kleinman *et al* speculated the specific siRNA for AMD treatment might not have been delivered into the cell (Kleinman, Yamada et al. 2008), therefore suggesting the urgent need of proper siRNA delivery systems. Here will be presented the review of current art of RNAi delivery below this section.

1.5.4 Two basic strategies for RNAi delivery

As described in the previous section, RNAi activity follows two pathways: 1) siRNA triggered by the exogenous viral RNA or dsRNA, or 2) miRNA that is produced by intracellular processing of longer hairpin transcripts (Fig. 1-4). While direct delivery of naked RNAi is low in efficiency and economically unfavorable, facilitated delivery strategies take advantage of the two pathways and can be characterized as RNA-based and DNA-based. The RNA-based approach of RNAi delivery utilizes the former pathway, where dsRNA/ssRNA can be transported to the host cell by forming a complex with synthetic vectors: liposome complex (Gilmore, Fox et al. 2006; Aagaard and Rossi 2007), cationic polymers (Gilmore, Fox et al. 2006), cholesterol conjugation (Rossi 2004), nanoparticle capsule (Hogrefe, Lebedev et al. 2006), cell penetrating peptide attachment (Chiu, Ali et al. 2004), and antibody conjugation (Rossi 2005; Sioud 2006). DNA-based approach, on the other hand, mimics the miRNA pathway by inserting a viral vector (also know as viral-based approach) to the host genome in order to produce the pre-miRNA in the nucleus.

1.5.5 Problems of the gene silencing delivery system

An important challenge in gene therapy is the need for an acceptable and efficient delivery system that has minimal toxicity and maximum patent safety. In general, the interfering effect of an RNA-based approach is transient and intrinsically less stable compared to those from viral-based methods. Viral vectors, however, introducing viral protein to the host while delivering the gene of interest, may cause unsolicited immune response. Recently the death of the patient who received adeno-associated virus (AAV) gene therapy for arthritis treatment has raised public concern about using viral vectors (Check 2003; Kaiser 2007).

On the other hand, toxicology involving the modulation of gene expression by chemicals or other RNAi delivery agents is of high concern. Studies show that cationic lipids can reduce cell proliferation (Lawrencia, Mahendran et al. 2001) and initiate immune system responses (Marques and Williams 2005). Polypropylenimine (PPI) dendrimer (branch-like structure polymer), a popular cationic polymer for the delivery of nucleic acids, was found to alter the expression of several endogenous genes (Omidi, Hollins et al. 2005). Since the early reports by Ambrose and Moroson in 1950s and 1970s, many more polymers have been reported to directly or indirectly promote anti-tumor activity via stimulation of the immune system. Of direct relevance to RNA gene silencing are recent studies showing that the immunostimulatory effect of certain RNA motifs is dependent on the use of lipid or polymer delivery systems (Marques and Williams 2005). These studies showed that drug delivery systems induce a wide range of transcriptional changes in cells including cytokines and apoptosis signaling pathways (reviewed by Akhtar (Akhtar and Benter 2007)). These findings highlight the importance of the delivery system and the biological effects of RNA interference in developing a useful RNAi therapy.

1.5.6 Plant viruses as vaccines

Target molecules can be engineered into plant virus vectors and produced as vaccine antigens or as a fused epitope displayed on the viral coat protein. Studies on these plant-made-vaccines (PMV) have shown successful results on animal disease control, such as malaria and rabies (Ashraf, Singh et al. 2005). One of the major attractions of having plant made vaccine is the possibility of oral delivery. Leafy feed and food crops have been used for vaccines antigen production including alfalfa, lettuce,

and spinach. Despite these positive achievements, negative public opinions on genetically modified crops and the concern of gene leakage to the environment deferred the first USDA approved PMV for market until January 2006 (Vermij 2006). Non-crop species like tobacco, as shown in the USDA approved case, are favorable options because they minimize the regulation barriers regarding entry into the food chain. The leaves are harvested before flowering to reduce the spread of pollens or seeds to the environment. In fact, tobacco and *Tobacco mosaic virus* are now the most common plant and plant virus species used for the production of vaccine antigens (Joensuu, Niklander-Teeri et al. 2008).

1.6 The model proteins for RNAi study: cyclin E and EGFP

CycE is endogenously regulated by the cell cycle mechanism and is highly related to cell growth. In this study, RNA interference is utilized to target cyclin E translation as well as cell cycles. The dysfunction of the cell cycle checkpoint has emerged as a frequent and pivotal cause of genetic instability; therefore, the chance of the unstable cells to develop cancer will increase. Since cyclins, Cdks, and CKIs plays key roles in cell cycle control, the efforts to regulate these cell-cycle-related molecules will be potential cancer therapies.

In addition, enhanced green fluorescent protein (EGFP) is selected as another model protein to exam the TMV RNAi delivery system. EGFP has excitation and emission peaks at 488nm and 507nm, respectively, compared to its wild type form (wtGFP) of Ex:395nm and Em:509nm. EGFP was designed to be brighter and have an excitation peak matching that of an argon laser, which is commonly used with fluorescent activated cell sorters (FACS). The variant is optimized for mammalian expression by the addition of a Kozak consensus translation initiation site at the beginning of the gene (Haas, Park et al. 1996), the deletion of potentially inhibitory sequences, and the inclusion of 190 silent mutations using preferred human codons (Cormack, Valdivia et al. 1996; Yang, Cheng et al. 1996). GFP and its variants have been the most popular biomarker used in cell biology and in other biological disciplines such as cell imaging, and protein expression for their suitability of real-time detection. EGFP in this study is chosen as a visual biomarker to be expressed in a transgene in a stable cell line and antisense *EGFP* RNA is delivered to suppress EGFP translation.

1.7 Objectives

The scheme of experimental design for this project is presented in figure 1-8. TMV virions will be disassembled followed by coat protein recovery. The stripped TMV RNA will be reverse-transcribed to produce a copy of cDNA which will then be inserted into an *E. coli* plasmid for DNA recombination. Genes of interest, antisense EGFP and antisense cyclin E, will be incorporated with the TMV cDNA plasmid for RNA synthesis. Once the recombinant RNA is made, the previously separated TMV coat protein will be added for the pseudo virion re-assembly. This synthesized virion can be either decorated for receptor-mediated endocytosis or assisted by transfection agents (e.g. cationic liposome) for cell entry. The ssRNA is expected to be released from TMV coat protein to form RISC for post-translational suppression.

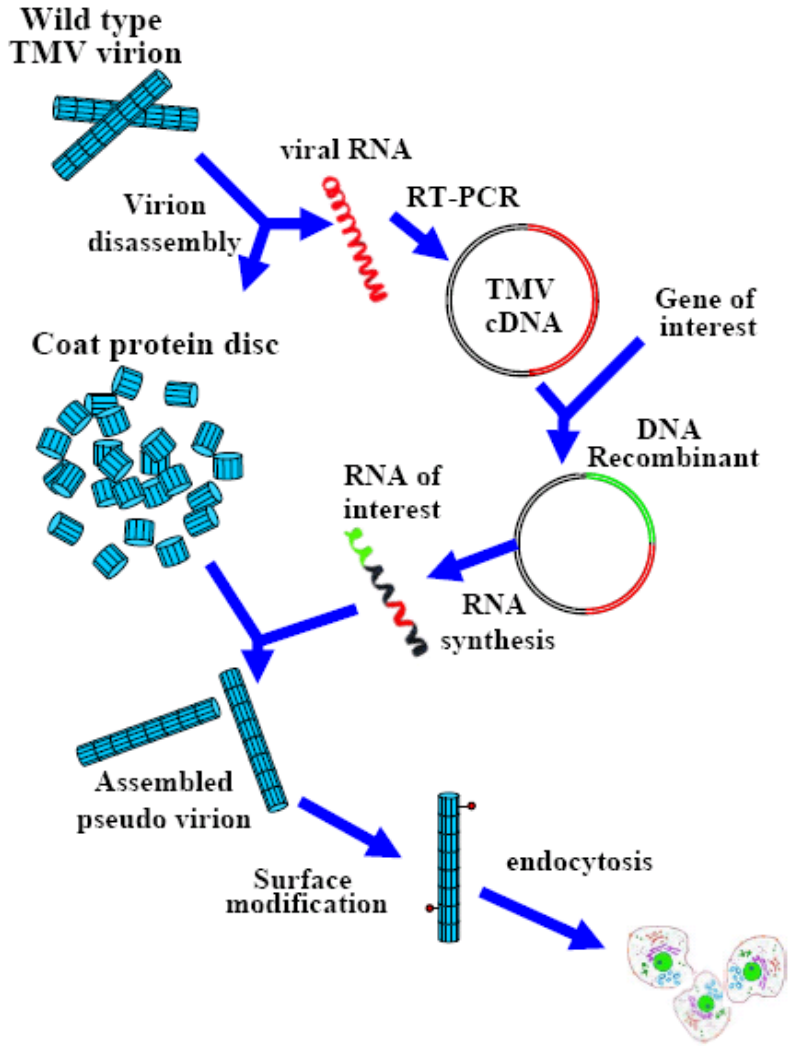

Figure 1-8 Scheme of the experimental design in this work

As the procedure stated, the hypotheses of this research are as follows:

1. RNA with TMV OAS will be encapsulated in TMV CP.
2. The re-assembled TMV pseudo virion will protect the encapsulated RNA from RNAse degradation.
3. The length of the re-assembled virion will be determined by the size of the RNA within.
4. The entry of TMV to the cell can be facilitated by 1) receptor mediated endocytosis – specifically by cell penetrating peptides, or 2) a cationic liposome.
5. Once endocytosed, the TMV virion will be dissembled in the cell and release the RNA for gene silencing.
6. The ssRNA released from TMV will be processed via siRNA pathway for gene silencing.
7. Cyclin E gene down-regulation will result in cell arrest in G1 phase and/or apoptosis.
8. *EGFP* mRNA down-regulation by RNAi will inhibit EGFP expression and reduce the fluorescence.

Chapter 2 of this work will present the endocytosis of TMV by cell-penetrating peptides while chapter 3 will illustrate the process of TMV disassembly and re-assembly for RNAi gene delivery. Finally, a discussion and a conclusion will be given in chapter 4.

2 HUMAN CELL ENDOCYTOSIS OF PLANT VIRUS

2.1 Endocytosis

The term "endocytosis" was first proposed in 1963 to define a combination of various means by which cells internalize extracellular material (de Duve 1963). Endocytosis takes part in many important physiological processes, including extracellular nutrient uptake, antigen presentation, glucose transport, cell polarity maintenance, and regulation of cell-surface receptor expression. It also presents an important way by which microorganisms and toxins get into cells. Disease processes that are related to abnormalities in endocytosis including prion diseases (i.e., Creutzfeld-jakob disease in humans, mad-cow disease in cattle) (Shyng, Heuser et al. 1994; Shyng, Moulder et al. 1995), Alzheimer's disease (Kang, Lemaire et al. 1987; Nordstedt, Caporaso et al. 1993; Koo and Squazzo 1994), and Atherosclerosis (Goldstein, Brown et al. 1985; Tabas 1995).

Based on the size of the material that is taken up by the cell, and the means by which it is transported through the cell membrane, endocytosis is divided into 3 major categories, phagocytosis, pinocytosis, and clathrin-dependent receptor-mediated endocytosis.

2.1.1 Phagocytosis

Phagocytosis was first defined in 1893 by Metchnikoff (Metchnikoff 1893). It is also known as "cell eating". It is a mechanism by which cells (e.g., neutrophiles, monocytes and macrophages in mammals) internalize large particles and microorganisms (Predescu, Horvat et al. 1994).

Phagocytosis is a receptor-dependent process, and the substance being transported is specific to a particular receptor. The receptors on cell surface can either recognize particles directly or through an opsonin coating on the particle, e.g., immunoglobin coating (Greenberg and Silverstein 1993). The main mechanism of internalization by phagocytosis is the so-called "zipper model" (Griffin, Griffin et al. 1975; Griffin, Griffin et al. 1976). In short, plasma membrane of a phagocyte cell extends two "pseudopods" to enclose the proximate particles being taken-up, in a zipper like manner. The pseudopods around the particle meet and fuse to form a phagosome with the particle engulfed inside (Swanson and Baer 1995). The phagosome then moves into cytosol to fuse with a lysosome forming a phagolysosome, and the particle inside gets degraded. Finally, the internalized membrane of the phagosome is recycled back to cell surface (Muller, Steinman et al. 1980; Muller, Steinman et al. 1983).

2.1.2 Pinocytosis

Pinocytosis discussed here refers to receptor-independent pinocytosis. It is also known as "cell drinking". During pinocytosis, an area of the cell surface buds into the cytosol to form a vesicle, which is small compared to phagosomes. Surrounding solutes and small single molecules, like proteins, which otherwise would be hard to get through the hydrophobic plasma membrane, are engulfed in vesicles. Vesicles then fuse with lysosome, and the molecules inside get degraded. Unlike phagocytosis, where transport is receptor dependent , the molecules taken up by pinocytosis are non-specific.

2.1.3 Clathrin-dependent receptor-mediated endocytosis

Clathrin-dependent receptor-mediated endocytosis, which will be referred to as RME (receptor-mediated endocytosis) in this section, was first described by Roth and Porter in 1964 (Roth and Porter 1964). It is the best understood and also the major endocytosis route in most cells. RME differs from pinocytosis in that it is receptor-mediated, via clathrin-coated pits.

Receptors are proteins on the outer surface of the plasma membrane. They possess binding sites for some specific molecules such as hormones, cholesterol and vitamins, which are low in concentration in the extracellular surroundings. Therefore, through receptors, these specific molecules can be selected to be internalized to meet cell needs.

Clathrin is a large, basket-like protein with a light chain and a heavy chain (Kanaseki and Kadota 1969). It is inlaid on the inner surface of the plasma membrane. Together with some other cytoplasmic proteins such as dynamin and adaptin, clathrin mediates the conversion of a budding pit to a vesicle. Once a vesicle is formed, clathrin is removed from the vesicle. Then, the vesicle moves into cytosol to fuse with an endosome, and the receptors are either recycled back to the cell surface, or sent to a lysosome to be degraded.

2.1.4 The role of some specific amino acid sequences in the LDL receptor

In 1985, it was first demonstrated that a natural tyrosine to cysteine mutation in human low-density lipoprotein (LDL) receptor impaired the RME of LDL (Goldstein, Brown et al. 1985). Further investigation revealed that a conserved sequence NPXY is essential for LDL internalization, that this NPXY is located in the cytoplasmic tail of the LDL receptor (Davis, Goldstein et al. 1987; Lobel, Fujimoto et al. 1989; Miettinen, Rose

et al. 1989), and that this specific cytoplasmic amino acid sequence is important in determining coated pit localization (Goldstein, Brown et al. 1985). A similar specific amino acid sequence, YXRF, was identified for the transferrin receptor (Jing, Spencer et al. 1990; McGraw and Maxfield 1990). The common theme is that an aromatic residue, usually a tyrosine, is required in the cytoplasmic tail, and polar or positively charged residues are preferred around the tyrosin.

2.2 Cell-penetrating peptide for gene delivery

Two decades ago, Green and Frankel showed the HIV-1 (human immunodeficiency virus serotype 1) Tat protein could enter the cell when added to the medium(Frankel and Pabo 1988; Green and Loewenstein 1988). It was soon clear that a peptide sequence from Tat, YGRKKRRQRRR, is essential to the trans-membrane activity. Since this initial observation, other proteins/peptides possessing the trans-membrane activity have been identified: the third α-helix of Drosophila Antennapedia (Antp) homeotic transcription factor(Joliot, Pernelle et al. 1991; Derossi, Calvet et al. 1996), VP22 of HSV(Elliott and O'Hare 1997; Phelan, Elliott et al. 1998), transportan(Pooga, Kut et al. 2001), polyarginine(Rothbard, Garlington et al. 2000; Wender, Mitchell et al. 2000), and adenovirus (ADV) fiber protein(Zhang, Andreassen et al. 1999). These cell-penetrating peptides, also known as membrane translocation signals(Lewin, Carlesso et al. 2000), protein transduction domains(Schwarze, Ho et al. 1999), and transfecting peptides(Zhang, Andreassen et al. 1999), are listed in Table 2-1.

Cell penetrating peptide	Peptide sequence
HIV-1 TAT	YGRKKRRQRRR
HSV VP22	DAATATRGRSAASRPTERPRAPARSASRPRRPVE
ADV fiber protein	KRARPSEDTFNPVYPYDTET
ANTP	RQIKIWFQNRRMKWKK
Transportan	AGYLLGKINLKALAALAKKIL
Poly arginine	RRRRRRRRRR

Table 2-1 Cell-penetrating peptide sequences. Amino sequences stated in this research are from N terminus to C terminus.

The mechanisms of these cell-penetrating peptides for internalization are still unclear. It is noteworthy that ADV fiber protein contains NPVY (table 2-1), the RME sequence for LDL, which may suggest its RME pathway for internalization. However, the fact that ADV fiber protein loses its activity on membrane translocation at 4^{o}C (Tkachenko, Xie et al. 2003) while Tat and VP22 retain efficient protein transduction at that temperature (Derossi, Joliot et al. 1994; Vives, Brodin et al. 1997) seems to indicate that Tat and VP22 use different pathways than RME. Also, confocal studies of the mechanism of Antp and Tat bound peptide show that the time course of uptake and their cellular distribution does not correlate with transferrin, another RME protein (Jones, Christison et al. 2005). These results suggest that cell-penetrating peptides use various pathways for endocytosis.

Regardless, these cell-penetrating peptides have been popular in gene delivery for membrane translocation. Tkachenko *et al.* showed that inert gold particles, when complexed to a peptide corresponding to adenovirus RME sequence, NPVYPYEDESKKKKKC, can efficiently pass through the HepG2 cell membrane(Tkachenko, Xie et al. 2003), suggesting the fundamental role of the specific sequences in RME. Furthermore, in the same study they also showed that when gold nanoparticles are simultaneously complexed to both adenovirus RME sequence and adenovirus nuclear localization signal (NLS) sequence, AKRARLSTSFGGC, or even one longer peptide containing both RME and NLS sequences (AKRARLSTSFNPVYPYEDESKKKKKC), the gold nanoparticles could not only cross cell membrane through an RME pathway, but also escape the lysosomal pathway, and target the cell nucleus (Tkachenko, Xie et al. 2003).

In this research the cell-penetrating peptides will be used to facilitate TMV for human cell entry. Specifically the peptides discovered by Tkachenko *et al.* will be chemically crosslinked to the TMV surface to aid the virion in HEK293 cell entry. The procedures will be provided in the following section.

2.3 Materials and Methods

2.3.1 TMV virion purification

TMV virions, both wild-type (U1) and mutant 1cys, were isolateded from infected *N. tabacum* cv. Xanthi leaves and purified as described by Gooding and Hebert (Gooding and Hebert 1967). Virus was further purified by ultracentrifugation at 25,000 rpm (Beckman rotor SW28) and quantified by absorbance (King and Perham 1971). TMV1cys is a genetically modified strand from wild type U1 where a single cysteine residue was added to the N-terminal of each wild type TMV coat protein (Yi, Nisar et al. 2005).

2.3.2 Bifunctional crosslinker : SPDP

N-Succinimidyl-3-(2-PyridylDithio)-Propionate (SPDP) (from Pierce, IL) was used as a crosslinker to conjugate the cell-penetrating peptide to the TMV virion by covalent bonds – specifically the cysteine residue on TMV1cys and the amine residue on the cell-penetrating peptide. Two synthetic peptides labeled with rhodamine, 1) NLS (AKRARLSTSFGGG, rhodamine on lysine, Invitrogen) and 2) RME3 (NPVYPYEDESKKKKK, rhodamine on the terminal lysine, Invitrogen), were tested as

cell-penetrating peptides. TMV (500 mg) in 300 μL phosphate buffered saline (pH 7) was mixed with SPDP (670 nM, 10μL stock solution in DMSO) and incubated for 30 min in the dark at 22^{o}C (room temperature) for surface activation. The two peptides of 5μL described above (NLS and RME3, 6.7 nM) were added respectively to the activated TMV buffers and incubated in the dark for another 30 min to complete surface modification.

2.3.3 Density gradient for TMV recovery

Sucrose density gradients were utilized for TMV recovery after surface modification. Sucrose (25% w/w, in PBS buffer, pH 7), was frozen and thawed to form a density gradient of approximately 10% to 40%. The peptide-TMV samples were carefully loaded onto the sucrose gradient followed by ultracentrifugation at 28,000 rpm for 2 hr at 4^{o}C (Rotor SW50.1, Beckman). Control experiment of fluorescein-5-maleimide labeled TMV was performed as a reference in centrifugation. The fraction of the fluorescent TMV was pelleted in de-ionized water to remove sucrose. The resulting TMV was resuspended in 200 μl de-ionized water.

2.3.4 Mammalian cell culture

HEK293 cells (human embryonic kidney cell, ATCC number: CRL-1573) were cultivated in Dulbecco's Modified Eagle's Media (DMEM) containing glucose (4.5 g/L), GlutMAX™ I (3.97 mM), and 10% fetal bovine serum (FBS, Sigma) at 37^{o}C in a 6 well plate till the cell density reached 1x10^{6} cell/mL. The medium was replaced by 2mL of DMEM without the addition of FBS. Surface modified TMV samples of 20 μL were

then added to the cell culture for endocytosis and incubated at 37°C for another hour. The medium was changed back to DMEM supplemented with 10% FBS for another 8 hr before harvesting for confocal microscopic observation.

2.3.5 Confocal Microscope

HEK293 cells were trypsinized for 5 min at 37°C, collected by centrifugation at 500 g, and resuspended in phosphate buffered saline (pH 7.2). The cells were loaded on the glass slide and examined with a confocal microscope (Zeiss LSM510) with HeNe laser (Ex: 543nm) for the detection of rhodamine (610nm).

2.4 Results and Discussion

2.4.1 Cell-penetrating peptides bound covalently to TMV virion

For plant viruses to be internalized into mammalian cells, wild-type TMV virions, which have no cysteine on outer surfaces, will need some modifications to their coat protein. TMV1cys was genetically created by insertion of a cysteine residue to be displayed on the outer surface(Yi, Nisar et al. 2005). As a result, covalently attaching other molecules to TMV surface was made possible via this additional thiol group from cysteine(Lee, Royston et al. 2005; Yi, Nisar et al. 2005).

SPDP was utilized to covalently bind the cell-penetrating peptide to TMV1cys. Hetero-bifunctional crosslinker SPDP contains reactivity toward amines through the succinimide group, and toward sulfhydryls as well through a pyridylthiol group. TMV1cys was first activated by attaching SPDP to the cysteine residue, followed by the addition of rhodamine labeled, cell-penetrating peptide RME3 (NPVYPYEDESKKKKK) or nuclear localization signal NLS (AKRARLSTSFGGG). These peptides were synthesized with an attached rhodamine so that they could be recognized either visually or by confocal microscopy.

2.4.2 Ultracentrifugation to separate the TMV from unreacted peptide

The peptide-TMV mixture was loaded onto the sucrose density gradient for separation. Fluorescein labeled TMV was used here as the experimental control for TMV separation. Figure 2-1 shows the results after centrifugation. Both RME3 and NLS peptides can bind to the TMV1cys, and the peptide-bound TMV can form a separated zone from the un-reacted peptide.

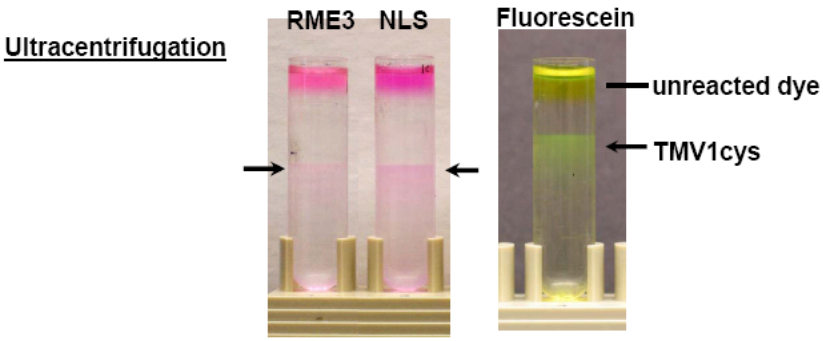

Figure 2-1 Ultracentrifugation to purify peptide-bound TMV. Left: two rhodamine labeled peptides, RME3 and NLS, were covalently bound to TMV1cys. After density gradient centrifugation, peptide-bound TMV1cys, shown in red fluorescence, can be separated from the un-reacted peptide (on the top). Right: fluorescein-labeled TMV1cys was used as a reference here.

It is noted that a band of green fluorescence was formed from the sample with fluorescein-bound TMV in the centrifuge tube (Fig. 2-1 right). The peptide-bound TMV, however, created a smeared red-fluorescent section from the middle section of the tube down to the bottom (Fig. 2-2, left), indicating that the conjugation of the TMV virions might occur by the crosslinker, SPDP. Since SPDP is capable of crosslinking both amines and thiols, TMV1cys, possessing both groups on the outer surface, might be conjugated by SPDP to form virion aggregates – which leads to the smeared red band in the density gradients.

On the other hand, the crosslinking reaction was carried out by changing the reaction sequences – by mixing the peptide and SPDP first, followed by the addition of TMV. This reaction worked on peptide NLS, but was problematic on peptide RME3 because each RME3 molecule has a penta-lysine (amine) tail where each lysine is able to bind SPDP. Once more than one lysine on the RME3 molecule was activated by SPDP, the RME3-SPDPs complex could react to several TMV virions, resulting in TMV agglomeration and precipitation. Thus, the reaction sequence as stated in the materials and methods (TMV-SPDP-RME3) is preferable to the reaction sequence RME3-SPDP-TMV.

The centrifugation was able to separate TMV from the un-reacted peptide. Red fluorescent fractions were collected from the middle section of the centrifuge tube, followed by cell culture tests on the peptide-bound TMV for human cell endocytosis.

2.4.3 Cell-penetrating peptide facilitated human cell endocytosis of TMV

In order to test cell-penetrating peptide facilitated human cell endocytosis, RME3-bound TMV and NLS-bound TMV were added to the DMEM medium on HEK293 cells. In six hours, the cells were harvested by trypsin and washed twice with PBS buffer to minimize the peptides attached to the cell membrane. The suspended HEK293 cells were observed under a confocal microscope for red fluorescence. Figure 2-2 is the confocal images and western blot analysis of the HEK293 cell samples. Under microscope, red fluorescence was detected on HEK293 transfected with RME3-bound TMV (Fig. 2-2b), but not on the NLS sample (Fig. 2-2c). In addition, z-stack analysis showed that the red-fluorescence was located inside the cell membrane, illustrating that the peptide was taken up by the cell. HEK cells in Fig 2-2a had no detectable natural red fluorescence, acting as a negative control in this experiment.

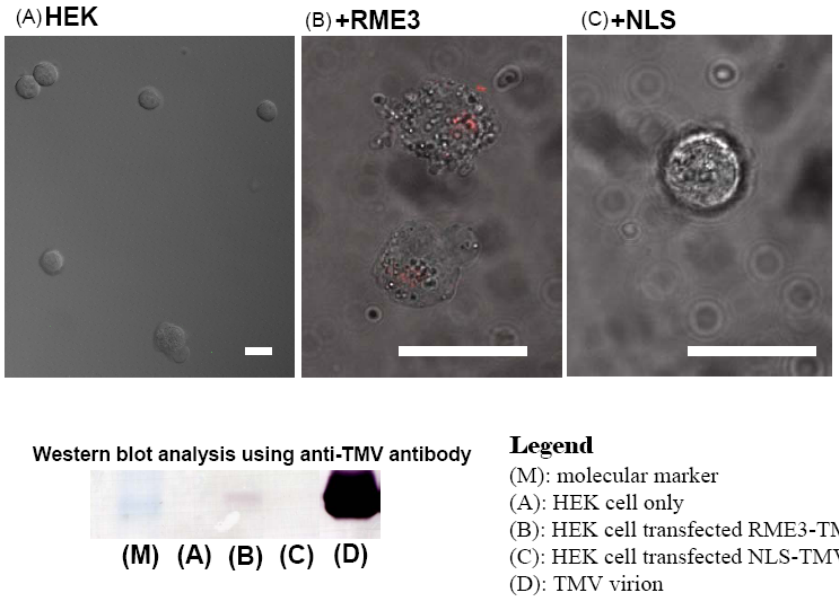

Figure 2-2 HEK cells' endocytosis of peptide bound TMV. Three confocal images on the top shows (A) HEK cells only, (B) HEK cells transfected with RME3 peptide, and (C) HEK cells transfected with NLS peptide. Based on the red fluorescence, only peptide RME3 was allowed cell entry. HEK Cells Peptide NLS was not able to enter the HEK cell. Image on the bottom shows a western blot analysis of the corresponding samples using anti-TMV CP antibody. The western blot analysis indicated positive results on (B) HEK cell transfected with RME3-TMV, and (D) TMV virion (positive control), which agrees with the confocal observation. White scale bars represent 5μm.

Immunoblot results (western blot) on the sample lysates for TMV CP specific antibody agreed with the confocal studies. Shown at the bottom part of Fig. 2-2 is the western blot result where lanes (a)-(c) are loaded with corresponding cell lysate samples in the top part of Fig. 2-2. Lane (d) is the western blot positive control loaded with wtTMV virion. The western blot confirmed that the peptide bound TMV was endocytosed, and the red fluorescence was not from the degraded rhodamine or peptide alone.

2.4.4 Concluding remark : peptide RME3 can facilitate cell endocytosis

These experiments supports the conclusion that peptide RME3 was able to facilitate the endocytosis of TMV into HEK293. According to a previous study (Tkachenko, Xie et al. 2003), peptide NLS was only able to direct translocated material (DNA/RNA/nanoparticles) to the cell nucleus oce in the cytoplasm. Thus, the NLS is a signal peptide for penetrating the nuclear membrane while RME3 is a peptide for crossing cytoplasmic membrane. This mechanism of cell-penetrating peptide-mediated endocytosis can later be applied for TMV-based RNAi gene delivery.

3 RNA PACKAGING AND GENE DELIVERY USING TMV PSEUDO VIRIONS

In the previous chapter, TMV has been surface-engineered to possess cell-penetrating peptides that help the plant virus enter human cells. In this chapter, TMV will be utilized as a gene carrier that delivers RNA interference to cells. Fig. 1-8 shows the scheme of the experimental design of this work.

3.1 Materials and Methods

3.1.1 Coat protein subunit preparation

TMV virion, both wild-type (U1) and mutant E50Q, were isolateded from infected *N. tabacum cv.* Xanthi tissue and purified as described by Gooding and Hebert (Gooding and Hebert 1967). Virion was further purified by ultracentrifugation at 25,000 rpm (Beckman rotor SW28) and quantified by absorbance at 260/325nm (King and Perham 1971). E50Q is a genetically modified strand from wild type U1 so that glutamic acid (E) #50 was replaced by glutamine (Q) (Lu, Stubbs et al. 1996). This replacement disrupted the carboxyl-carboxylate interaction between CP subunits, so that wild type TMV virions treated with excess E50Q CP were greatly inhibited in their ability to disassemble both *in vivo* and *in vitro* (Lu, Stubbs et al. 1996). Purified coat protein of both wild-type and E50Q subunits were prepared as described by Fraenkel-Conrat (Fraenkel-Conrat and Williams 1955; Fraenkel-Conrat 1957), and concentrations were determined by microchip electrophoresis (Protein 230 Assay, Agilent Technology). The coat protein was prepared in 0.05M sodium phosphate buffer of various pH. Transmitted

electron microscopy (TEM) was performed by stabilizing the coat protein onto formvar-coated grids and staining the samples with 1% of uranyl acetate.

3.1.2 Plasmid construct and RNA synthesis *in vitro*

A full length infectious cDNA clone of the U1 strain of TMV, pSNC007, was used as a parental construct for all derivatives in this study (Dawson, Beck et al. 1986; Turpen, Reinl et al. 1995). Specifically, the plasmid possessed a phage T7 promoter at 5' end and a hammerhead ribozyme at 3' end of the TMV cDNA. Once transcribed, the RNA product would self-process at the ribozyme cleavage site and would be uniform in size (Turpen, Turpen et al. 1993)(Fig. 3-1).

EGFP DNA was extracted by PCR from plasmid pEGFP-N1 (Clontech) using primers 1 and 2 (Table 3-1). The PCR fragment was first digested with XmaI and SacII, then ligated with the corresponding unique site on pSNC007, disrupting the 126 kDa ORF. The resulting plasmid was named pX752 (Fig. 3-1).

Plasmid pX763, which contains an full length of antisense EGFP sequence, was constructed in the same manner using primers 3 and 4, and ligated into the XmaI-SacII sites of pX752 (Fig. 3-1). In addition, TMV OAS was extracted from pSNC007 by primers 5 and 6, digested with SacII and BsiWI, and cloned into the corresponding sites of pX763. This plasmid, pCHEGFPi, possessing antisense EGFP sequence under the T7 promoter, would be effectively shorter (1600 nt) than pX752 or pX763 (4700 nt) once the encoded RNA was transcribed (Fig. 3-1).

CycE antisense DNA was extracted from High Five™ cell (BTI-TN-5B1-4, Invitrogen) cDNA by PCR using primers 7 and 8. The cDNA was prepared by reverse transcriptase polymerase chain reaction (RT-PCR) using the RNAqueous Kit (Ambion),

and the SuperScript III first strand Synthesis system (Invitrogen) with a non-gene specific primer (oligo dT). The PCR product carrying the antisense *CycE* sequence was cloned into the XmaI-SacII sites of pCHEGFPi. The resulting plasmid is named as pDTCycEi for *CycE* RNA interference (Fig 3-1).

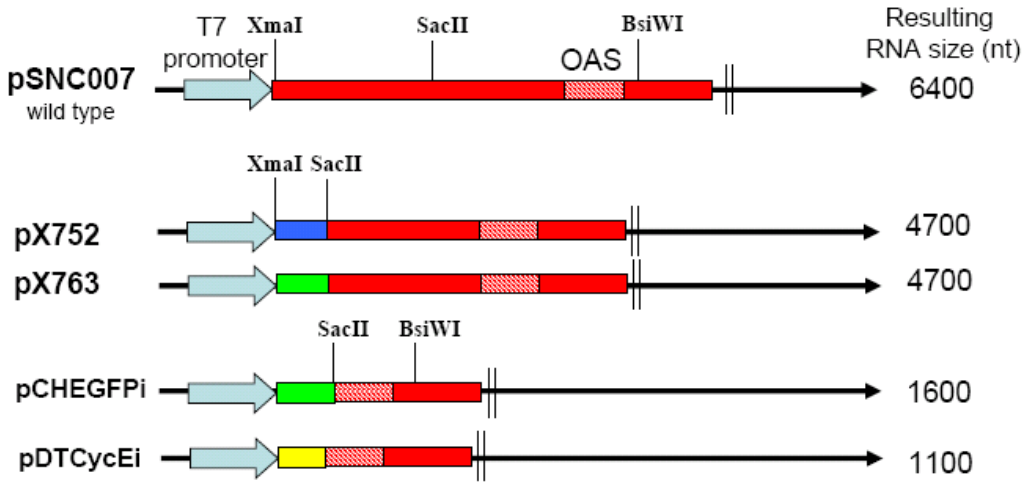

Figure 3-1 Plasmid constructs in this work. With T7 promoter at the 5' end and a ribozyme at 3' end of the wild type (U1) TMV cDNA, the transcribed RNA from pSNC007 is the full length TMV RNA of 6400 nt. Plasmid pX752, by replacing part of the 126 kDa ORF with *EGFP* sequence (blue), retains the OAS (patterned red) from pSNC007 and will produce RNA size of 4700 nt. Plasmid pX763 is constructed by replacing the *EGFP* gene (blue) with antisense *EGFP* sequence (green). pCHEGFPi is a shortened version of pX763 by extracting the OAS via PCR and inserting the OAS back to pX763 at SacII and BsiWI sites. This will effectively shorten the RNA product from plasmid pCHEGFPi. Plasmid pDTCycEi is constructed by replacing the antisense EGFP (green) in pCHEGFPi with antisense *CycE* (yellow). Legend: Red, TMV sequence; Blue, *EGFP* sequence; Green, antisense *EGFP* sequence; Yellow, Cyclin E sequence (*CycE*); double straight line, ribozyme; Red patterned, origin of assembly sequence(TMV OAS).

Table 3-1 Primers used in this study.
Underlined sequence indicates endonuclease digestion sites: XmaI (CCCGGG), SacII (CCGCGG), or BsiWI (CGTACG).

Primer #	Function	Sequence
1	Extracting EGFP, forward primer for PCR to make pX52	5’ - CTA ACC CGG GAT ATG GTG AGC AAG GG - 3’
2	Extracting EGFP, reverse primer for PCR to make pX52	5'- CTG ACC GCG GTT TAC TTG TAC AGC TCG - 3'
3	antisense EGFP, forward primer for PCR extraction	5' - GCG CCC CGG GAT GTA CAG CTC GTC CAT GC - 3'
4	antisense EGFP, reverse primer for PCR extraction	5' - CGC GCC GCG GTA TGG TGA GCA AGG GCG - 3'
5	Extracting OAS, forward primer for PCR to make pCHEGFPi	5’-TCC CCG CGG TCT GGT GGA CAA AAG GAT GG – 3’
6	Extracting OAS, reverse primer for PCR to make pCHEGFPi	5’- GTC AAC GTA CGG TTC TTG TTC GGC ACT GAC C – 3’
7	antisense *T. ni* Cyclin E, forward primer for PCR extraction	5' - TCC CCC CGG GTA AGA TCT CGT CTG TG - 3'
8	antisense *T. ni* Cyclin E, reverse primer for PCR exaction	5' - TCC CCG CGG ACT GGC TGA ATG AGG - 3'
9	Sf actin forward primer for RT-PCR loading control	5' - GAT ATG GAG AAG ATC TGG CA - 3'
10	Sf actin reverse primer for RT-PCR loading control	5' - GCG TAG CCC TCG TAG ATG - 3'
11	CycE forward primer for RT-PCR; detecting CycE mRNA depletion	5' - TTC CGC GTT ACC GTG TTG ACT A - 3'
12	CycE reverse primer for RT-PCR; detecting CycE mRNA depletion	5' - CGG ATT GTC TGA GTG GTC CAT ATC CG - 3'

3.1.3 RNA *in vitro* synthesis

The *E. coli* plasmids mentioned above were isolated from cell culture by the miniprep kit (Qiagen kit) to serve as templates to synthesize RNA. Purity and quantity were checked by OD260/280nm. RNA was synthesized *in vitro* using the transcription kit (MEGAScript High Yield Transcript Kit, Ambion) under guidance of the manufacture's protocol. The transcribed product was then purified using a spin column (Qiagen RNeasy Mini Kit) and treated with DNase (DNase I, 25^{o}C, 30 min) to remove the plasmid DNA. The purified, DNA-free RNA products were characterized by a microchip electrophoresis (RNA nano 6000, Agilent Technology) for their size, and also by polymerase chain reaction (PCR) for 30 cycles to ensure that the sample is free of plasmid DNA contamination. The quantified RNAs, denoted as rX752, rCHEGFPi and rDTCycEi, were stored in DEPC-treated water and were ready for virion assembly.

3.1.4 Pseudo virion assembly

Coat protein (400 μg) was added to the synthesized RNA (20 μg) in 0.05 M sodium pyrophosphate buffer at pH 7 at 20^{o}C and incubated for 16 hr to promote virion assembly. The assembled virion product was treated with RNase A and DNase I for 1 hr at room temperature to remove the un-reacted nucleotides, followed by ultracentrifugation.

3.1.5 Ultracentrifugation to separate virions from CP, nucleases, and RNAs

Once the disc CP was mixed with ssRNA the virions formed spontaneously. The next step was to separate the assembled virions from the un-reacted CP, RNA and other nucleases. This can be achieved by either: 1) size exclusion chromatography, or 2)

density gradient centrifugation. In this study, the later method was chosen because the sample was very limited (~200μL). Specifically the density gradient was performed by loading the RNase-treated virion sample onto a 5mL, approximately 10-40% sucrose density gradient solution, which is made by freezing and thawing 25% of sucrose solution. Similar centrifugal setup, formed by loading fluorescein-labeled TMV onto the second sucrose gradient, was performed with the virion setup and centrifuged at 28,000 rpm (Beckman rotor Ti 50) for 3 hr as a reference. The virion sample was fractionated and collected every 600μL from the top, labeled as f1 to f8 (f1 from the top). Unfolded TMV CP and bare RNA were retained on the top part of the tube (f1). Each fraction was diluted with deionized water to 5mL and centrifuged at 22,000 rpm again for an additional 30 min. The supernatant was carefully removed and the pellet was resuspended in 10μL of sodium phosphate buffer at pH 7. Each of the 10μL concentrated virion sample was stained as described previously for electron microscopy to verify the assembly of the virion. The assembled pseudo virions were found in the f4 sample.

3.1.6 RNA extraction from the assembled virion

The assembled virion was tested for its ability to protect the encapsulated RNA from RNase degradation. Virion sample was first diluted with 10mM Tris buffer, pH 8.0 and RNase A was added to a final concentration of 0.1 μg/mL, incubating at room temperature for 1 hr. Following the RNase A treatment was the addition of excess protease K (0.5mg/mL, final concentration) in order to quench RNase A and dissemble the virions. The proteolytic reaction was carried out for an additional 30 min at room temperature, followed by phenol/chloroform/SDS extraction with an additional 5 μg of carrier tRNA to facilitate RNA precipitation (as memtioned previously by (Gaddipati,

Atreya et al. 1988)). The RNA, collected by ethanol precipitation and resuspended in water, was analyzed by RT-PCR to check its integrity and to verify the protection of the TMV coat protein.

3.1.7 Self-assembled virion and its cellular responses

The pseudo-virion, with its 126 kDa replicase sequence from TMV disrupted, possesses no infectivity to plants (reviewed by Buck (Buck 1999)). The assembled virion, however, carried a single stranded RNA to be tested for its RNA interference ability. Two virion samples, vCHEGFPi and vDTCycEi, were tested for their ability to inhibit the corresponding gene expression, namely *EGFP* and *cycE*. Two eukaryotic cell lines, HEK293 (human embryonic kidney cell, ATCC no: CRL-1573) and High Five insect cells, were used respectively as host cells to test vCHEGFPi and vDTCcyEi.

3.1.8 Virion vCHEGPi tested for EGFP interference

HEK293 cells were cultured in Dulbecco's Modified Eagle's Media containing glucose (4.5 g/L), GlutMAX™ I (3.97 mM), and 10% fetal bovine serum (FBS, Sigma), and were subcultured every two to three days in 75cm^2-tissue culture flasks (Costar) as the population approached 80-90% confluency. The cells were cultured onto a 6-well plate (Costar) prior to transfection (1 million cells per well).

Plasmid pEGFP-N1 (Genebank accession #: U55762, Clontech) and the assembled virion vCHEGFPi were transfected sequentially into HEK cells using a commercially available transfection reagent (Fugene^{TM} HD , Roche Applied Science). Plasmid pEGFP-N1 (50ng) was mixed with 7 μL of fugene and de-ionized water to make a final volume of 100 μL. The mixture of the plasmid and the fugene was incubated at

22°C on the benchtop for another 5 min before adding to HEK cell (100 μL per well). The cells were incubated at 37°C for 24 hrs before pseudo-virions were added for gene silencing. Virions vCHEGFPi (200ng), were diluted with DEPC-treated water and mixed with 7 μL of fugene to a final concentration of 100μL. Again, after 5 min the 100μL of virions was added to the cells in each well. Plasmid EGFP-N1 carried an *EGFP* gene under CMV promoter for EGFP transient expression in mammalian cells. Virions vCHEGFPi, possessing an antisense *EGFP* RNA, was used here to down-regulated the EGFP.

EGFP transfected cells were cultured for additional 12 hours before testing their fluorescence. For cell harvesting, HEK cells were trypsinized (1.5 mL Trypsin/EDTA, 5 min, 37°C), centrifuged (500 x g, 5 min, 25°C (RT)) and resuspended in 1mL PBS buffer. The green fluorescence was measured by a FACSCalibur™ (BD Biosciences, Immunocytometry) flow cytometer equipped with a 15 mW, 488 nm, air-cooled argon-ion laser, which was kindly provided by K. Frauwirth (University of Maryland, College Park). Data were analyzed using FlowJo software (Tree Star).

3.1.9 Virion vDTCycEi for Cyclin E interference

High Five cells were grown on ExCell 405 medium (JRH Bioscience) at 27°C and were subcultured every three days in a 75 cm^2 tissue culture flask. Cells were cultured to a 6-well plate prior transfection.

Assembled Virion vDTCycEi, which carried an antisense High Five *CycE* RNA, was transfected into the High Five cells using Fugene as a transfection reagent. The virion (200 ng) was diluted with DEPC-treated water and mixed with 7μL of fugene to a final volume of 100μL. The treated virion was incubated on the benchtop for 5 min

before added to the High Five cell culture. The cells were incubated at 27^{o}C for 16 hr (16 hpt, hours post transfection) and were collected by 0.25% trypsin-EDTA and resuspended in PBS, followed by propidium iodide staining. High Five cells in 1mL PBS were added dropwise to 4 mL ethanol for fixation and incubated on ice for 20 min. The cells were collected by centrifugation (500xg) and resuspend in 0.5 mL of propidium iodine (PI) solution (PI: 50μg/mL, RNase A: 0.1mg/mL, 0.05% Tritin X-100). The cell were stained with PI solution at 37^{o}C for 40 min before collected with centrifugation and resuspended with 500μL of PBS. Red fluorescence of PI was measured by FACSCalibur flow cytometer with 488nm argon laser in channel FL2 (585/42 nm), and data were analyzed using software FlowJo.

3.2 Results

Presented in this study is a self-assembled plant virion system to act as an RNA vehicle. The result of the study on the chimeric virus particles includes two major sections: the characterization of the viral particles and the application of the virus as an RNA vehicle. Coat proteins and ssRNA, the two basal materials that make the chimeric virus, will be first characterized in terms of their morphology and length respectively. After assembly, the length of the assembled virion will be compared to the length of the enclosed ssRNA. The assembled virion will also be tested for its ability to encapsulate and protect the ssRNA by performing reverse transcriptase PCR.

3.2.1 The characterization of the viral particles

3.2.1.1 Pseudo-Virion assembly

TMV coat protein (CP) changes its shape as pH and ionic strength changes (Durham, Finch et al. 1971). Without RNA present, the coat protein stacks up to rod-like structure at pH 5, disc-like at pH 7, and randomly aggregate to so-called A protein at pH 8 (Fig. 3-2). The surface charge on the CP, which varies with pH, leads to the morphological change of the CP. We noted that the rod-like structure can extend up to several microns without RNA at pH 5. This stacking process of the coat protein is spontaneous, and can be well controlled by adjusting pH in the buffer.

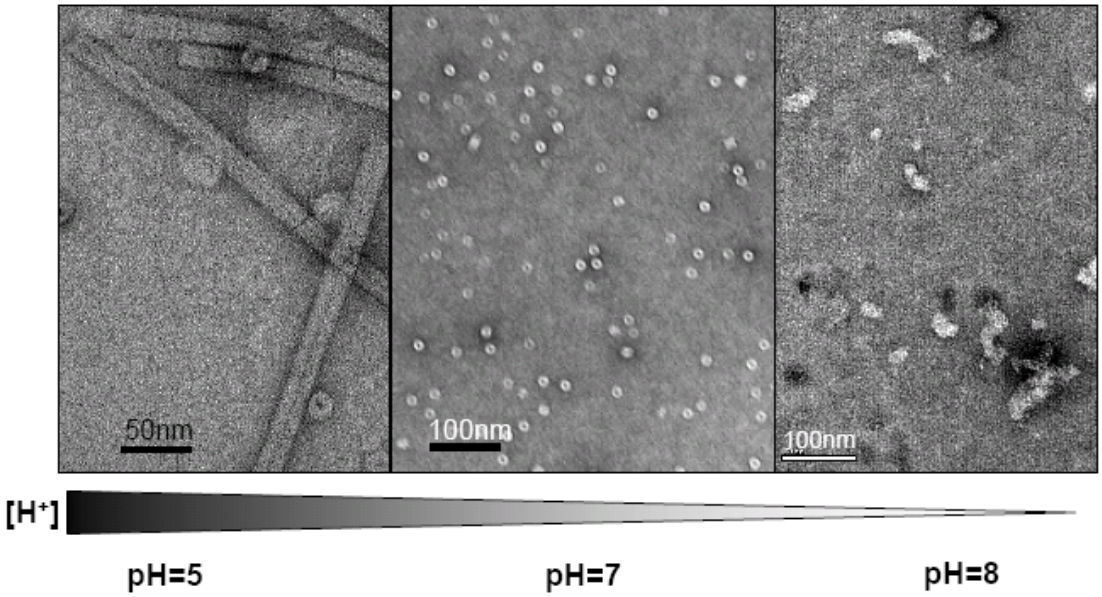

Figure 3-2TMV CP presents differently in morphology as pH changes. Left: TMV CP in sodium acetate 0.05 M, pH 5; Middle: TMV CP in sodium phosphate 0.05 M, pH 7; Right: TMV CP in sodium phosphate 0.05 M, pH 8.

Pseudo-virion assembly occurred when OAS ssRNA was added to TMV CP (pH 7, Fig. 3-3). Testes are four RNAs in different lengths (rSNC007:6400nt, rX752:4700nt, rCHEGFPi:1600nt, and rDTCycEi:1100nt) under microchip electrophoresis shown in figure 3-3A. These RNAs were *in vitro* synthesized under a T7 RNA polymerase promoter and could undergo self-cleavage at their ribozyme to minimize the random terminations of the RNA synthesis. These 4 RNA samples, though different in size, possess one significant feature in common: the OAS from TMV RNA which is essential for virion assembly.

Specifically, TMV cDNA (6395 bp) was used as a template to produce ssRNA of ~6400 nt (lane 2, Fig. 3-3A). It is known that wild type TMV virion is 300 nm in length (Fig 3-3B) which encloses the RNA of ~6400 nt . RNAs of different lengths (lane 3-5, Fig. 3-3A) were produced by various plasmid constructs (as described in Materials and Methods) and were tested for virion assembly. The ssRNAs (in DEPC treated water) were added to the TMV CP at pH 7 (in 0.05M sodium phosphate, disc form, Fig. 3-2 middle). In 16 hours, the rod-like pseudo virions were formed and examined by EM (Fig. 3-3C-E). The rod-like virion was not observed on the TMV CP sample added to RNA without OAS (data not shown).

Assembled rod-like virions from RNA samples pDTCycEi and pX752 were further analyzed for the size distribution by software ImageJ (Fig. 3-3D and 3-3E). Plasmid pDTCycEi was designed to produce ssRNA of 1100nt, while plasmid pX752 was to make ssRNA of 4700nt. The projected length of the virion produced from those two RNA samples would respectively be 50nm and 220nm while wild type TMV (300nm,

6400nt) was used as a standard scale. The size distribution of those two samples was shown in Fig. 3-4.

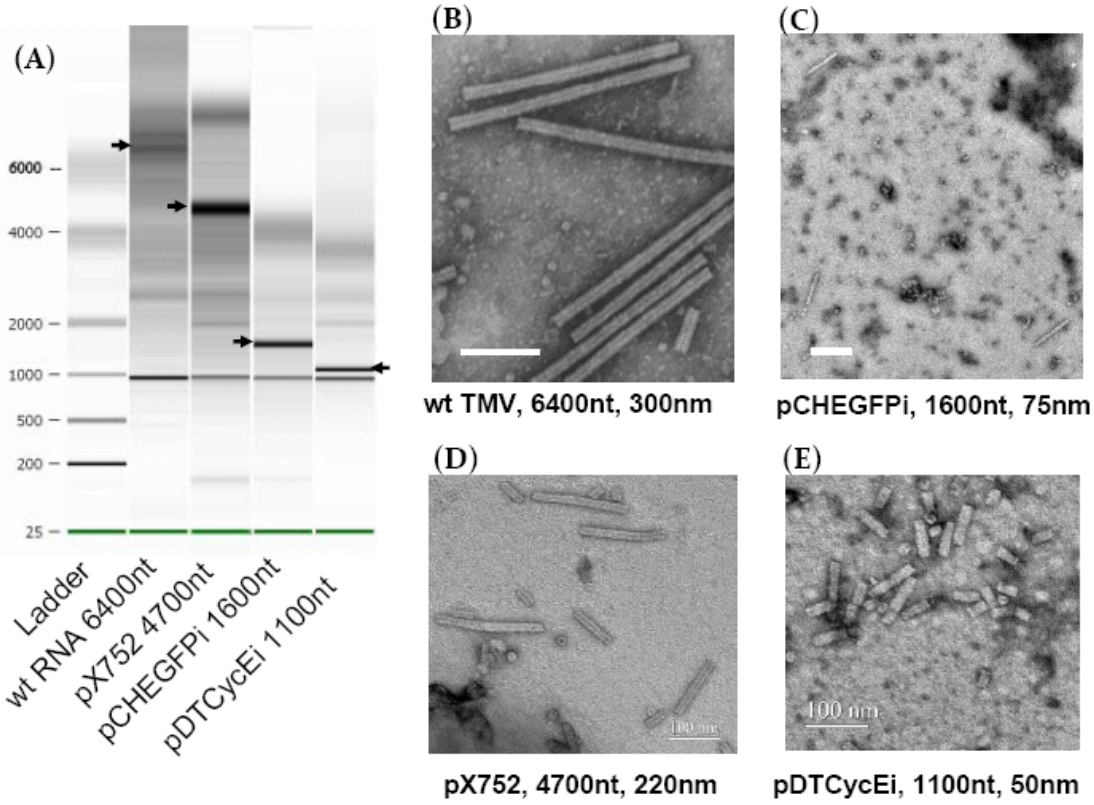

Figure 3-3 The lengths of a variety of RNA and their assembled virion. (A) The length of the RNA (6400nt, 4700nt, 1600nt, and 1100nt) was verified by the microchip electrophoresis; (B) wild type TMV virus (300nm) under EM (original virus, not re-assembled); (C)-(E), the EM images of re-assembled pseudo-virion with RNA different in lengths. The projected length of the rod encapsulating an ssRNA of 4700nt, 1600nt, and 1100nt would be 220nm, 75nm, and 50nm respectively when using wild type TMV (6400nt, 300nm) as a starndard. (White bar = 100nm)

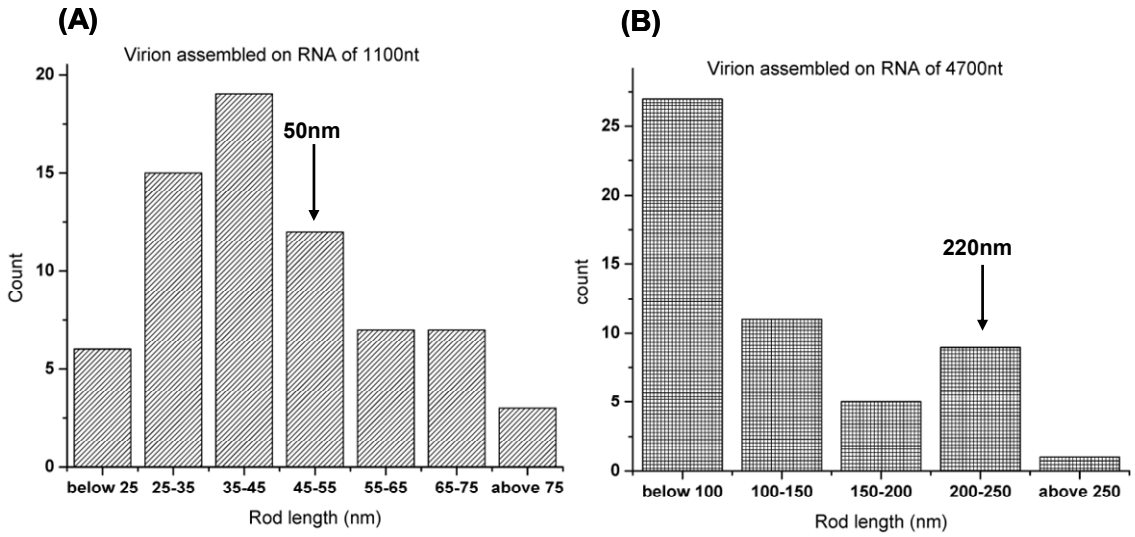

Figure 3-4 Assmebled virion length distribution on various RNA samples from rDTCycEi (left, 1100nt) and rX752 (right, 4700 nt). Wild type TMV, well known for its structure (300 nm), is composed of 6400 nt and coat protein. Using wtTMV as a scale, RNA of 1100nt and 4700nt would assemble into pseudo virion of 50nm and 220nm, respectively. On x-axis 25-35 denotes $25 \leq x < 35$.

3.2.1.2 Pseudo-virion size distribution

Electron microscope images of virion vX752 and vDTCycEi were analyzed by software ImageJ for size distribution. For each sample, 5 images were analyzed and all rods on the 5 images were counted unselectively and summed for size distribution. Again, the virion sample prepared with RNA rDTCycEi were expected to have rod length of 50 nm. Out of 70 rods counted, the average and median of the rod size is 46 nm and 43.5 nm, respectively. The size distribution in Fig. 3-4A showed that 45% of the rods are within the range of 35-55 nm.

For virion sample from vX752, the expected rod length was 220 nm. The observed rod length in sample vX752 was significantly larger than the previous one, where no rod over 100 nm was found (Fig. 3-4A). Although more than 50% of the population of vX752 is less than 100 nm, we observed another peak on the size distribution at 200-250 nm (Fig. 3-4B). The "two-peak" phenomenon in vX752 was not seen in the previous samples vDTCycEi. The right peak resulted from the virion assembly on the longer RNA; in fact, few discs were observed in the pX752 sample (Fig 3-3D), indicating the CP might be the limiting reagent to completely encapsulate all ssRNA.

We have shown that TMV CP changes its shape at different pH. At pH 7, TMV CP formed discs and allowed ssRNA with OAS to associate and assemble into pseudo virions. The size distribution of the assembled virions agreed with the size of the RNA within to initiate the rod formation. In the section following, the assembled virions would be tested for their biological properties both *in vivo* and *in vitro* for gene delivery purposes.

3.2.1.3 Virions to protect RNA from degradation

The following experiment was performed to demonstrate the protection of RNA by treating the assembled virions with RNase and DNase. Shown in Fig. 3-5A is the experimental design for virion assembly and nuclease test. First, the ssRNA were synthesized in vitro using T7 RNA polymerase with three DNA plasmids as templates—pX752, pDTCycEi, and pCHEGFPi, producing ssRNA of 4700 nt, 1600 nt, and 1100 nt, respectively. The RNA synthesis reaction lasted for 6 hr, followed by DNase I treatment to eliminate DNA contamination. Previously in Fig. 3-3A, the synthesized ssRNAs were tested by the microchip electrophoresis for their sizes. In this section, RT-PCR was performed on the ssRNA rX752 to check the integrity on the gene of interest as a positive control (Fig. 3-5, sample 2). To ensure the rX752 sample was free of DNA, PCR (with primer, Table 3-1) was performed as a negative control (Fig. 3-5, sample 1). Multiple DNase I treatments may be necessary to completely remove plasmid DNA contamination. In addition, rX752 was also treated with RNase, followed by RT-PCR (shown in Fig 3-5, sample 0). The fact that sample 0 had no signal demonstrated that ssRNA was subjected to RNase digestion if not protected (another negative control). Briefly, samples 0, 1 and 2 concluded that RNA of interest was successfully synthesized *in vitro*, the RNA product were DNA free, and the bare ssRNA is vulnerable to RNase degradation.

(A)

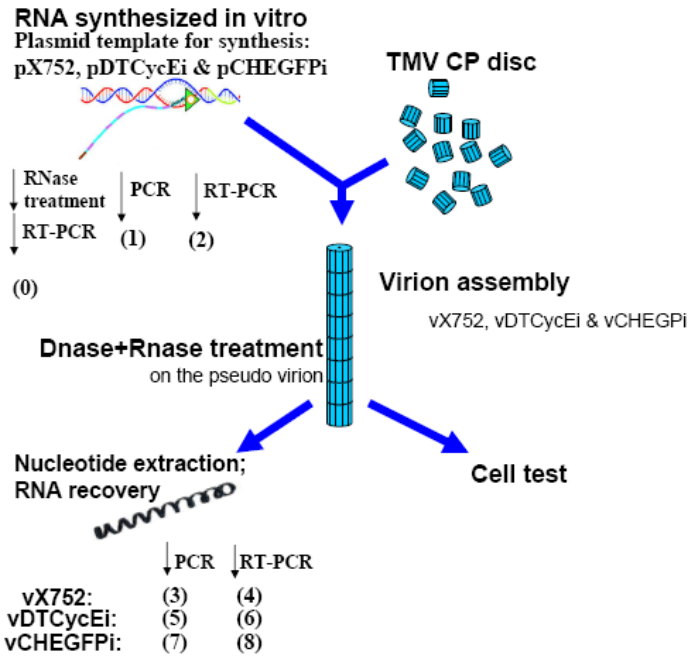

(B)

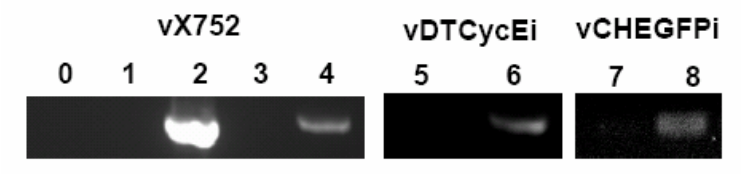

Figure 3-5 RT-PCR to exam the integrity of RNA enclosed in the virion. (A) Experimental scheme for virion assembly; (B) Electrophoresis of agarose gel on PCR and RT-PCR samples. Sample numbers in (B) correspond to those indicated in (A). Sample 0: RT-PCR on vX752 RNA sample which was pretreated with RNAse; Sample 1: PCR on RNA sample synthesized from plasmid pX752; Lane 2: RT-PCR on RNA sample synthesized from plasmid. Sample 3: PCR product from nucleotide extraction of vX752; Sample 4: RT-PCR product from nucleotide extraction of vX752. Samples 5 and 7 are repeated experiments from sample 3 with different plasmids, pDTCycEi and pCHEGFPi, respectively. Samples 6 and 8 are repeated experiments from sample 4 with different plasmids, pDTCycEi and pCHEGFPi, respectively.

Single strand RNA was then mixed with TMV CP (disc form) for virion assembly. In 16 hours, TMV CP enveloped the ssRNA and the virions were formed. The mixture containing CP, bare RNA, and newly-formed virions was treated with DNase I and RNase A to challenge the RNA integrity in the rods. Unenclosed RNA would be degraded as shown in sample 0. To recover the RNA, excessive protease K was added to quench the RNase and DNase before performing phenol/chloroform nucleotide extraction with 1% SDS.

The extracted vX752 RNA were tested again via PCR and RT-PCR for the existence of DNA and RNA, respectively (Fig 3-5B, sample 3 and 4). While no signal on sample 3 (PCR, vX752) indicated that no DNA was present (negative control), a clear band on sample 4 (RT-PCR, vX752) suggested the protection of the RNA in the virion sample due to TMV CP addition.

Using different plasmids (pDTCycEi and pCHEGFPi) as the templates to produce ssRNA, we tested the protection of TMV CP with different ssRNA. The bands on samples 6 and 8 are RT-PCR products which showed the RNA had been protected and were able to be recovered from virions vDTCycEi and vCHEGFPi, respectively. Samples 5 and 7, similar to sample 3 as the negative controls, had no signal on PCR, indicating no DNA was present on virions vDTCycEi and vCHEGFPi.

For ssRNA carrying no TMV OAS, the virion assembly did not happen and the RNA was not enveloped (data not shown). Single strand RNA possessing TMV OAS were able to associate with the TMV CP, producing rod-like pseudo virions, and protecting RNA from RNase/DNase digestion.

The pseudo virions have demonstrated their ability to protect the RNA within. The tests that followed will be the virion delivery to the host cells to exam the RNA interference activity.

3.2.2 Application of the pseudo virus as a RNA vehicle

3.2.2.1 EGFP RNA interference activity of TMV pseudo virions, vCHEGFPi

HEK293, as a host cell to test EGFP RNAi activity, was transfected with plasmid pEGFP-N1 for EGFP transient expression. Pseudo virions vCHEGFPi, enveloping ssRNA of 1600nt, were co-transfected into HEK293 cells with the EGFP producing plasmid, pEGFP-N1. The ssRNA within the vCHEGFPi contained an antisense strand of *EGFP* of 700nt, which could target the mRNA from pEGFP-N1 to form a dsRNA for gene silencing. Other factors that could affect the EGFP expression including TMV CP, RNase existence, bare ssRNA of antisense EGFP, transfection reagent Fugene, were also tested along with pEGFP-N1.

Flow cytometry analysis was performed 36 hr after transfection in order to test the EGFP expression and the inhibitory effect of vCHEGFPi (Fig. 3-6A). HEK 293 cells were tested as a negative control in the flow cytometer. HEK 293 cells with transfection reagent Fugene and HEK 293 cells co-transfected with TMV CP both showed the same fluorescence profile as the negative control (HEK293 cell only). For the cells with pEGFP-N1, 32% of total 10,000 cell counted was green fluorescent (GFP+) (Fig. 3-6A), which was regarded as the positive control and normalized to 1 (100%) (Fig. 3-6C). The data showed that the addition of RNase, bare ssRNA of rCHEGFPi, and purified vCHEGFPi were all able to inhibit the expression of EGFP on HEK293 cell by 38%, 63%, and 61%, respectively. To test the disassembly of virion in the cell, excessive E50Q mutant CP was added to the vCHEGFPi virion (virion: E50Q = 20ng : 100ng).

This E50Q mutant can also inhibit GFP expression by 52% (Fig. 3-6B and C). The results will be discussed later in this chapter.

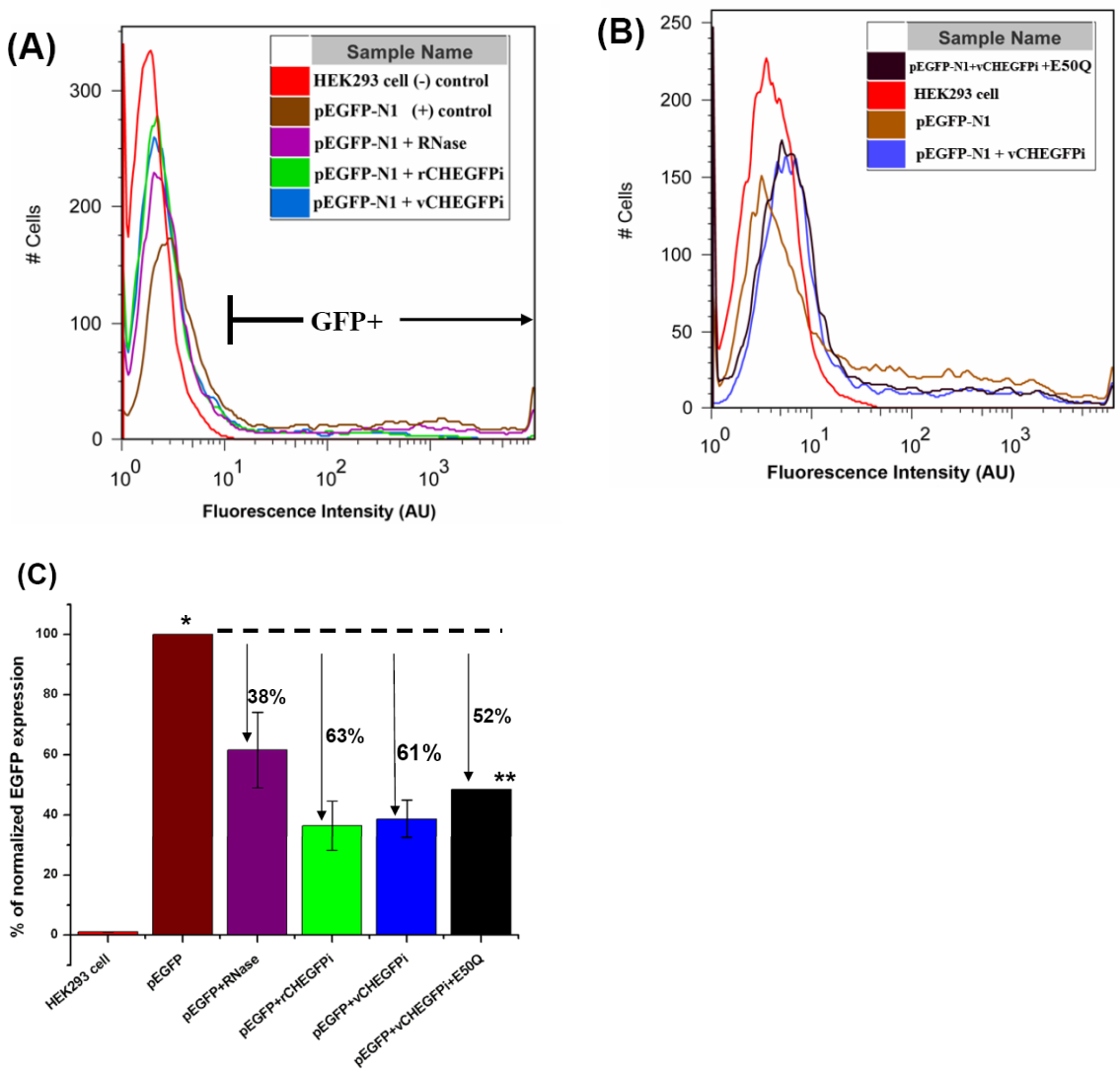

Figure 3-6 EGFP expression measured by flow cytometry. (A) HEK cells (red, negative control), HEK cells transfected with pEGFP-N1 (dark red, positive control), HEK cells cotransfected with pEGFP-N1 and Rnase (purple), HEK cells cotransfected with pEGFP-N1 and rCHEGFPi (green), and HEK cells cotransfected with pEGFP-N1 and vCHEGFPi (blue) were tested for the inhibition of EGFP. Cells possessing more than 15 (AU) in fluorescence intensity were considered as GFP positive. (B) To test the CP mutant E50Q, this vCHEGFPiE50Q was tested with other 3 samples for the EGFP inhibitory effect. HEK cells (red, negative control), HEK cells cotransfected with pEGFP-N1 (dark red, positive control), HEK cells cotransfected with pEGFP-N1 and vCHEGFPi (blue) and HEK cells cotransfected with pEGFP-N1 and vCHEGFPiE50Q (black). (C) The experimental results in figure A and B are summaried to figure C by quantify the GFP displaying cells. Rnase addition was able to reduce EGFP expression by 38%, bare ssRNAi was able to inhibit expression by 63%, pseudo virions 61%, pseudo virions with E50Q 52%.
*HEK cell transfected with pEGFP-N1 was regarded as positive control and normalized to 1 (100%).
**E50Q data set represented only one experiment. No error bar is available.

3.2.2.2 Cyclin E RNA interference activity of TMV pseudo virion vDTCycEi

High Five cells were used as the host cell to determine *cycE* RNAi activity. The cells were seeded on the 6-well plate at $1x10^6$ cell/well, and transfected with bare ssRNA of 1100nt, which contains 250 nt of antisense RNA from High Five cyclin E gene. The antisense of the *cycE* RNA can couple with the mRNA within the cell and down-regulate the gene via regular RNAi pathway, which is expected to arrest the host cells in G1 phase of the cell cycle.

3.2.2.3 RT-PCR results to test the gene silencing on RNA level

Previously in the test of *EGFP* RNAi, the phenotype change was observed by means of fluorescence inhibition. In the cyclin E test, the level of mRNA change induced by RNAi can be tested by RT-PCR. High Five cells were tested with the addition of rDTCycEi and vDTCycEi for cycE gene silencing. In addition, wild type coat protein and transfection agent fugene were also examined as control sets. Figure 3-6 shows the RT-PCR results from these High Five cells extract with different additions. Two electrophoresis images on the top are the RT-PCR results using primers to detect mRNA of actin (A) and *cycE* (B). The bottom chart in Fig. 3-6C is to quantify the intensity in the cycE RT-PCR, which represents the cycE mRNA in the cell. Since actin mRNA is transcribed constitutively and constantly in each cell, the mRNA of actin (Fig 3-6A) is used as loading control for normalizing the intensity in different samples. Lanes 1-7 represents the High Five cell will 1) fugene, 2) fugene + rDTCycEi, 3) fugene + vDTCycEi, 4) wild type CP, 5) nothing else (cell only), 6) rDTCycEi, 7) vDTCycEi, and 8) wild type CP. That only lane 2 and 3 showed the silencing of cyclin E shows both

single strand RNA rDTCycEi and pseudo virions vDTCycEi were able to knockdown cycE gene expression. Also these molecules required fugene for cell entry to take effects.

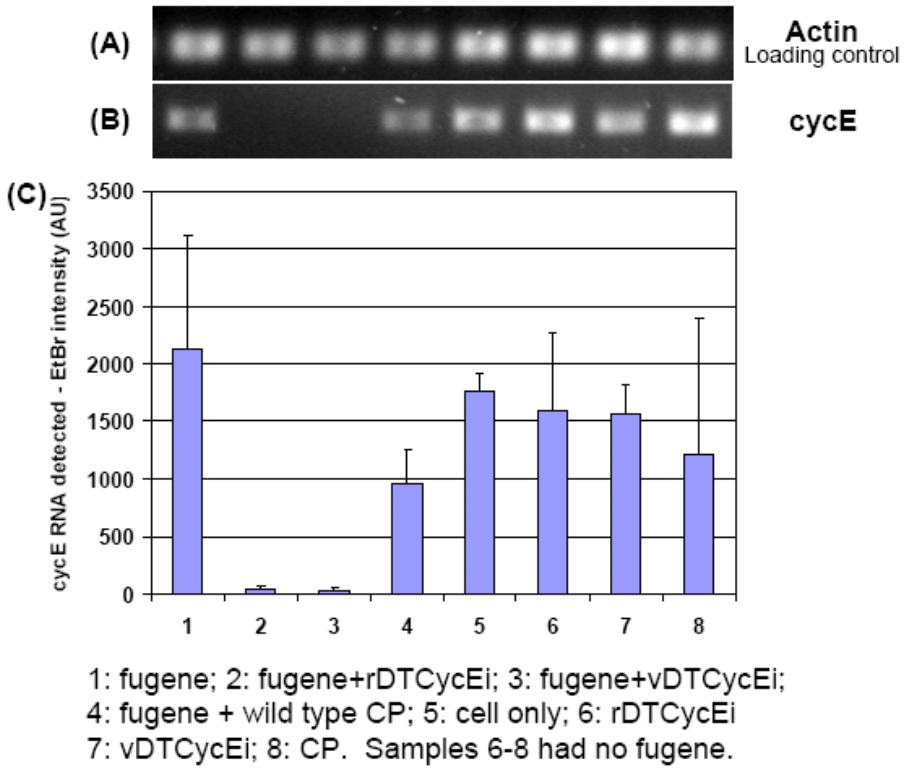

Figure 3-7 RT-PCR to test the inhibition of Cyclin E RNA by vDTCycEi. Two electrophoresis images represent the RT-PCR results detecting actin mRNA (A) and *cycE* mRNA (B) in the cytoplasm. The chart in (C) is the quantification of RT-PCR product intensity on cycE (B) of the corresponding sample. Lane 1: cells with transfection agent (fugene), lane 2: cells with fugene and rDTCycEi, lane 3: cells with fugene and vDTCycEi, lane 4: cells with wild type coat protein, lane 5: cells only, lane 6: cells with rDTCycEi (no fugene), lane 7: cell with vDTCycEi (no fugene), and lane 8: cells with coat protein (no fugene). The results indicated that both rDTCycEi and vDTCycEi with transfection agent were able to silence Cyclin E mRNA in the High Five cells. Actin is a constitutive gene served as a loading control in RT-PCR.

3.2.2.4 Cell cycle analysis on High Five cell for Cyclin E knockdown

In the previous section, RT-PCR results showed that by delivering antisense *CycE* RNA, the Cyclin E mRNA was down-regulated. In this section, cell cycle analysis will be conducted to confirm the influence of cycE knockdown.

High Five cell samples from lane 3 and 5 in Fig. 3-6 were used here for cell cycle analysis. Fig. 3-7A was the cell cycle analysis on regular High Five cells (also known as sample 5 in Fig. 3-6), where Fig. 3-7B was from sample transfected with vDTCycEi (sample 3 in Fig. 3-6). Sodium butyrate (NaB), a commonly used chemical to arrest cell in G1 phase(Abramova, Pospelova et al. 2006), was applied here as a positive control.

The cell cycle analysis by propidium iodine staining indicated that 58% of regular cells were in G1 (Fig.3-7A). By applying vDTCycEi, the G1 phase cell can increase to 61% (Fig. 3-7B), while chemical NaB can bring the fraction of G1 up to 67% (Fig. 3-7C). The cell cycle change and the G1 arrest were not as dramatic as the *cycE* mRNA depletion in Fig. 3-6.

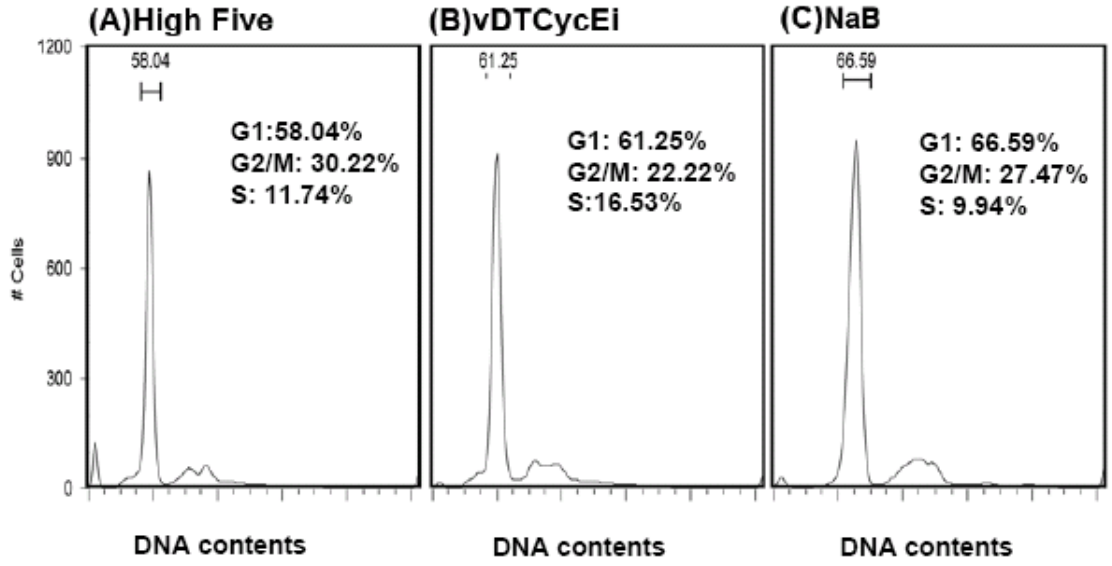

Figure 3-8 Cell cycle analysis for the High Five cells (A) High Five cells only (negative control), (B) High Five cells transfected with vDTCycEi, and (C) High Five cells with addition of 4mM of sodium butyrate (NaB, positive control for G1 phase arrest). The number indicated in the figures is the percentage of the cells in G1 phase. Virion DTCycEi can increase the G1 population from 58% to 61%, while cell treated with NaB has 67% of G1 population. In each case, 10,000 cells were counted.

3.3 Discussion

In this work, the results showed that CP aggregates into different forms in various pH (Fig. 3-2). The results from electron microscope also indicated that viral assembly can occur at pH 7 when discs were formed (Fig. 3-3).

3.3.1 Size distribution of assembled virions

The assembled virions changed their sizes with different sized RNA molecules. Wild-type TMV (300nm, 6400nt) was used as a reference to predict the size of the pseudo-virion. For an RNA of 1,100nt (rDTCycEi), the expected length of assembled virion was 50 nm. The average size of the assembled rod is 46nm (Fig.3-4A). No assembled rod more than 100nm was observed.

The assembled virions with RNA of 4,700nt (rX752) were expected to have a size around 220 nm. The majority of the virions observed under the EM were under 100nm. However, another peak on the range of 200-250 nm was observed in the size distribution (Fig. 3-4B).

The uncompleted assembly may be due to the insufficient amount of CP discs available, since fewer discs were observed in the EM image of the assembled sample (Fig. 3-3D). The nucleation (or assembly) process was terminated when CP discs were used up or when the full strand of RNA finished the viral assembly. The two-peak phenomenon in distribution suggested that the assembly process had different rate constants as the rod grew. The following model attempts to provide an explanation.

If we consider the rod growth as a process of the polymerization, the reaction can only react to one monomer (one disc) at a time because 1) the formation of a rod-like

structure (i.e. empty virion) at pH 7 by two empty discs (no RNA) is limited and can be omitted (Fig. 3-2), and 2) two discs that both have RNA inside do not polymerize with each other since the central holes on the discs are occupied. These assumptions lead to the conclusion that the polymerization reaction only occurs when one disc is activated by RNA to react to an empty disc.

Consider a series of polymerization reactions for virion assembly:

$$D + R \rightarrow D_1^*$$
$$D_1^* + D \rightarrow D_2^*$$
$$D_2^* + D \rightarrow D_3^*$$
$$\vdots$$
$$D_9^* + D \rightarrow D_{10}^*$$

where D: disc; R: RNA; D^*: Disc with RNA, as an activated disc that is capable of reacting with an inactivated D; subscript: number of monomers.

The virion length can also be considered as the molecular weight of the polymer, which increases as the polymerization proceeds. When the rate constant of the third reaction, for example, is lower than the first two, the intermediate dimer D_2, the product of the second reaction, is going to accumulate before finally being converted to the end product D_{10}. The polymerization ceases when CP disc is used up or when the end product D_{10} is formed. Therefore, the polymer size distribution will have two peaks – one on D_2 and another on D_{10}. The scenario matches our experimental results for the size distribution. In Fig. 3-4B, two peaks were observed: one corresponding to the short virions below 100 nm and the other corresponding to the accumulated end product at 220 nm.

Previous research shows the initiation and the elongation of the TMV assembly are two different mechanisms (Butler and Klug 1978). The experimental results in Fig. 3-4 suggest that the rate constant of the elongation is smaller than the one of the initiation.

3.3.2 Protection of RNA provided by TMV CP and the test of the RNA integrity by RT-PCR

The results in Fig. 3-5 showed that the enveloped RNA was protected from ribonuclease (RNase) degradation. RT-PCR was used in this experiment for verifying RNA integrity. RT-PCR is a powerful tool for detecting RNA by using the RNA of interest as a template to make the complementary DNA, followed by regular PCR. The downside is that RT-PCR detects DNA; therefore, DNA contamination will lead to a false positive result. In Fig 3-5, samples 1, 3, 5, and 7 were the control experiments where negative results on PCR illustrate that the samples are free of DNA. Sample 0, a negative result on the negative control, indicates that the RNA was subjected to RNase digestion. Samples 4, 6, and 8 show that enveloped RNA is preserved and can be recovered. Three RNAs (rX752, rDTCycEi, and rCHEGFPi) were tested in this experiment, indicating that the TMV-based RNA packaging process can be applied to different genes of interest.

3.3.3 Pseudo-virions targeting EGFP and Cyclin E for gene silencing

In this study of RNAi gene delivery, two genes of interest were chosen: 1) EGFP as a visual biomarker and 2) Cyclin E for cell cycle control. EGFP is expressed as a transgene in a stable cell line HEK 293, while Cyclin E is endogenously regulated by the High Five cells.

Pseudo-virions targeting EGFP (vCHEGFPi) were transfected into HEK293 cells by a transfection reagent, fugene. Experimental results showed that pseudo-virion, bare single-stranded RNA, and RNase could all inhibit the expression of EGFP (Fig. 3-6). RNase can unselectively digest RNA once in the cytoplasm, thus down-regulated any gene it encountered. RNase was selected in comparison with RNA and pseudo-virion (CHEGFPi) for *EGFP* gene silencing because initially the experiment was designed to have 1) pseudo-virion vCHEGFPi, 2) RNA rCHEGFPi, 3) pseudo-virion with RNase, and 4) RNA with RNase to test each one's ability to suppress EGFP. It is not surprising that both virion and antisense RNA can suppress EGFP. It was predicted that a less inhibitory effect on EGFP expression would be observed on the sample with RNA degradation by RNase treatment. However, the inhibitory effect did not subside as predicted because RNase alone can still suppress gene expression.

Pseudo-virions targeting *cycE* RNA were used to down-regulate cyclin E activity. Since cyclin E is essential to G1 to S checkpoint, the knockdown of cyclin E will cause cell arrest in G1. In this study, the population of G1 was increased from 58% (normal cell) to 61% (vDTCycEi, Fig. 3-7B). On the other hand, the positive control of NaB could only increase G1 population to 67%. Despite of the small increase in G1 population, the mRNA was depleted by the delivery of antisense RNA and pseudo-virions (Fig. 3-6B). Interestingly, previous studies show that cyclin E overexpression and knockdown can both induce apoptosis (Dhillon and Mudryj 2003; Gurzov and Izquierdo 2006). Our experimental results showed that, in addition to the change of the cell cycle, cell apoptosis was increased by 10% in the pseudo-virion sample, but not in the cell sample transfected with wtTMV (negative control, data not shown). Therefore, we

conclude that cyclin E was successfully down-regulated by pseudo-virions based on the facts that 1) *CycE* mRNA was depleted, 2) G1 population was increased, and 3) apoptosis was induced.

3.3.4 How does the TMV virion get disassembled in mammalian cells?

The observation of knockdowns on EGFP and Cyclin E gene shows that the ssRNA enveloped within the assembled virion was functional and was able to trigger RNAi activity on the RNA level and on the protein level. However, it is still not clear how exactly the ssRNA was released from the assembled virion within the cell.

In plant cells, TMV virions are disassembled due to the nature of physiological conditions - high pH and low Ca^{2+} that destabilize the interactions of CP-CP subunits and the interactions of CP-RNA. Structural studies of TMV have identified a switching mechanism provided by the intersubunit clusters of carboxyl-carboxylate groups from glutamic acid (E) or aspartic acid (D) located at the interface between adjacent CP subunits. Particularly the axial interaction between two negatively charged residues E50 and D77 can provide carboxyl-carboxylate repulsion to lead TMV disassembly. Under stabilizing conditions, the repulsive interactions made by the negatively charged carboxylate groups would be stabilized by the presence of positively charged calcium ions (Ca^{2+}) or protons (H^{+}). The mechanism of disassembly is initiated by the loss of the stabilizing ions due to high pH and low calcium ions in the plant cell. The mutant of E50Q reduces the repulsive charge between axial CP subunits so that the E50Q mutation stabilizes the TMV virion. In brief, the consequence of the point-mutated CP E50Q is that stable TMV virions keep RNA from releasing. A previous study showed that the

addition of mutant E50Q CP to wild type virus (10,000:1) reduced the TMV infectivity by 90%(Lu, Taraporewala et al. 1998).

In this study, E50Q CP was added to the assembled pseudo virions vCHEGFPi to form vCHEGFPiE50Q for *EGFP* gene silencing. E50Q was expected to keep the interfering RNA from releasing; therefore, the interfering activity was expected to subside. Experimental results showed that virion CHEGFPi was able to reduce EGFP expressing cells by 61% whereas vCHEGFPiE50Q was still able to reduce cells that displayed green fluorescence by 52%. The change of EGFP expression in HEK cells was not as dramatic as the change of infectivity in plant cells.

The fact that EGFP was down-regulated suggests that the RNA in the virion was released into the cytoplasm. However, when trying to use mutant E50Q to block the viral disassembly, the outcome was not supportive enough to make the conclusion that the disassembly process of TMV pseudo-virion in the human cells was initiated by the physiological nature of high pH and low calcium ions as in plant cells. To further explain how the virions are disassembled in the human cells, more experiments will be needed.

3.3.5 Coat protein enhances the flexibility in RNA delivery by surface modification

The current challenges of RNAi delivery are the instability of the RNA molecules and the lack of efficient RNAi delivery to target cells. The TMV-based RNA packaging system, shown in this study, was able to provide the protection to the enclosed RNA from degradation, and provides a variety of binding sites for further modifications. Importantly, attaching a functional group to RNA molecules for gene delivery is particularly difficult because RNAs are susceptible to degradation and the binding sites are at either end of the molecules. Enclosed in the pseudo virions, RNAs are protected

and the binding sites for modification greatly increase. TMV1cys, for example, has one RNA molecule with ~2000 cysteines for binding. The surface of the pseudo-virions brings flexibility for cell entry (as in this work), antigen display (e.g. vaccine), and other drugs to form complexes (e.g. nanoparticles). In addition, the coat protein in this study was chemically conjugated to the cell penetrating peptides. The surface display of peptides can also be achieved by genetically alteration on the coat protein (Staczek, Bendahmane et al. 2000) so that the chimeric virus can be produced by *N. tabacum* cv. Xanthi leaves without post harvest modification. In brief, a TMV-based RNA packaging system can provide protection to RNA and flexibility for modification for various purposes.

4 CONCLUSION

This study presents a RNA interference delivery system developed from the TMV assembly and disassembly mechanisms. First, the morphological change of TMV CP caused by the change of pH was studied for the virion assembly. The enclosed RNA was composed of the RNA of interest and the TMV OAS that promoted the assembly. Pseudo virion assembly occurred when the TMV CP (pH 7) was added to the RNA. The length of the resulting virions changed in agreement with the size of the enveloped RNA.

The assembled virions were tested in two aspects: 1) the ability to protect the RNA and 2) the ability to target gene silencing. Results illustrated a successful recovery of the RNA from the pseudo-virions after RNase treatment while a parallel experiment showed the bare RNA was subjected to RNase digestion. EGFP and Cyclin E were chosen as the model genes for the RNAi study. EGFP was transiently expressed by plamid pEGFP-N1 using CMV promoter in HEK cells while Cyclin E was endogenously regulated by the cell cycle mechanism in High Five cells. Assembled virions targeting *EGFP* mRNA was able to suppress EGFP expression by 61% whereas virions targeting *CycE* was capable of increasing G1 population from 58% to 61%.

The delivery system provides both the protection to the RNA and a variety of binding sites for surface modification. Results also showed that TMV1cys virions were capable of surface modification through a bifunctional crosslinker to covalently attach to cell penetrating peptides. These peptides helped transport TMV across the cell membrane. These two methods of producing self assembled virions and conducting

surface modification to the virions, when performed sequentially, can potentially create a cell targeting siRNA delivery system.

In summary, we presented a successful attempt to deliver the functioning pseudo-virions in the TMV-based non-viral siRNA delivery system. However, listed below are some problems of this delivery system that need to be stressed for improvement.

4.1 Limitations of the TMV based RNA delivery system

4.1.1 Low yield of cell penetrating peptides bound to pseudo virions

In chapter 2, the cell penetrating peptides RME3 was used to successfully facilitate TMV endocytosis. In chapter 3, cell entry of pseudo-virions by the transfection reagent effectively caused gene silencing. Due to the complexity of the crosslinking reaction, the yield for the RME3-bound TMV was 5-10%. In addition, the recovery rate of the pseudo-virion dis/assembly was 1-10%. The processes are yet to be optimized; therefore, the low yield and recovery rate make it a challenge to perform them sequentially – i.e., to produce pseudo-virions first followed by modifying the virion surface. For now, the transfection reagent can provide an immediate alternative for gene delivery into cultured cells while the delivery mechanism is optimized.

4.1.2 Intrinsic RNA backbone from TMV OAS may down-regulate other genes

In order to be enveloped by the pseudo virion, the RNA of interest was incorporated into the TMV OAS that initiated the assembly process. RNA rCHEGFPi, for example, contains an antisense *EGFP* sequence of ~700 nt and the backbone of the TMV OAS sequence of ~900 nt, resulting in a total length of 1,600 nt. The attempts to make pCHEGFPi from pX763 (Fig. 3-1) involved extracting the minimal part of OAS for

successful RNA packaging. This method reduced the size of the backbone from 3,800 nt (in pX763) to 900 nt (in pCHEGFPi) and the RNA products from pCHEGFPi and its derivatives were able to initiate virion formation. However, it is not clear whether the RNA of 900 nt can play any role in gene regulation in mammalian cells. The human genome database from Basic Local Alignment and Searching Tool (BLAST, http://www.ncbi.nlm.nih.gov/blast/Blast.cgi) has been used to search for similarity between human genome and TMV OAS backbone. We have found similarity of a 35-nt segment with Human chromosome 5 and another 34-nt segment with Human chromosome 10. We have yet to identify any gene silencing activities caused by the similar segments. RNA microassay may be suggested to further investigate this problem.

5 BIBLIOGRAPHY

Aagaard, L. and J. J. Rossi (2007). "RNAi therapeutics: Principles, prospects and challenges." Advanced Drug Delivery Reviews **59**(2-3): 75-86.

Abramova, M. V., T. V. Pospelova, et al. (2006). "G1/S arrest induced by histone deacetylase inhibitor sodium butyrate in E1A + Ras-transformed cells is mediated through down-regulation of E2F activity and stabilization of beta-catenin." J Biol Chem **281**(30): 21040-51.

Akhtar, S. and I. Benter (2007). "Toxicogenomics of non-viral drug delivery systems for RNAi: Potential impact on siRNA-mediated gene silencing activity and specificity." Advanced Drug Delivery Reviews **59**(2-3): 164-182.

Alberts, B., A. Johnson, et al. (2002). Checkpoints generally operate through negative intracellular signals. Molecular biology of the cell. New York, Garland Science**:** 992.

Arce-Johnson, P., U. Reimann-Philipp, et al. (1997). "Requirement of the Movement Protein for Long Distance Spread of Tobacco Mosaic Virus in Grafted Plants." Molecular Plant-Microbe Interactions **10**(6): 691-699.

Ashraf, S., P. K. Singh, et al. (2005). "High level expression of surface glycoprotein of rabies virus in tobacco leaves and its immunoprotective activity in mice." J Biotechnol **119**(1): 1-14.

Beck, M. and M. R. Strand (2003). "RNA interference silences Microplitis demolitor bracovirus genes and implicates glc1.8 in disruption of adhesion in infected host cells." Virology **314**(2): 521-35.

Beemster, G. T. S., F. Fiorani, et al. (2003). "Cell cycle: the key to plant growth control?" Trends in Plant Science **8**(4): 154-158.

Bertrand, J. R., M. Pottier, et al. (2002). "Comparison of antisense oligonucleotides and siRNAs in cell culture and in vivo." Biochemical and Biophysical Research Communications **296**(4): 1000-1004.

Bloomer, A. C., G. Bricogne, et al. (1978). "Structure of the Protein Disk of Tobacco Mosaic-Virus - Subunit Interactions and Implications for Virus Assembly." Acta Crystallographica Section A **34**: S396-S396.

Bloomer, A. C., J. N. Champness, et al. (1978). "Protein Disk of Tobacco Mosaic-Virus at 2.8-a Resolution Showing Interactions within and between Subunits." Nature **276**(5686): 362-368.

Buck, K. W. (1999). "Replication of tobacco mosaic virus RNA." Philosophical Transactions of the Royal Society of London Series B-Biological Sciences **354**(1383): 613-627.

Butler, P. J. G., A. C. Bloomer, et al. (1976). Tobacco mosaic virus assembly - specifity and the transition in protein structure during RNA packaging. R. Markham and R. W. Horne. Amsterdam, North Holland Publishing Co.**:** 101-110.

Butler, P. J. G. and A. Klug (1978). "Assembly of a Virus." Scientific American **239**(5): 62-69.

Buzzell, A. (1960). "Action of Urea on Tobacco Mosaic Virus." Journal of the American Chemical Society **82**(7): 1636-1641.

Canto, T., S. A. MacFarlane, et al. (2004). "ORF6 of Tobacco mosaic virus is a determinant of viral pathogenicity in Nicotiana benthamiana." J Gen Virol **85**(Pt 10): 3123-33.
Carthew, R. W. (2001). "Gene silencing by double-stranded RNA." Current Opinion in Cell Biology **13**(2): 244-248.
Caspar, D. L. D. (1963). "Assembly and Stability of the Tobacco Mosaic Virus Particle." Advances in Protein Chemistry **18**: 37-121.
Check, E. (2003). "Harmful potential of viral vectors fuels doubts over gene therapy." Nature **423**(6940): 573-4.
Chiu, Y. L., A. Ali, et al. (2004). "Visualizing a correlation between siRNA localization, cellular uptake, and RNAi in living cells." Chem Biol **11**(8): 1165-75.
Choi, C. W., S. H. Park, et al. (2000). "Chemical degradation of tobacco mosaic virus followed by infectivity assay, reverse transcription-polymerase chain reaction and gel electrophoresis." Acta Virologica **44**(3-4): 145-149.
Chuang, C. F. and E. M. Meyerowitz (2000). "Specific and heritable genetic interference by double-stranded RNA in Arabidopsis thaliana." Proc Natl Acad Sci U S A **97**(9): 4985-90.
Clemens, J. C., C. A. Worby, et al. (2000). "Use of double-stranded RNA interference in Drosophila cell lines to dissect signal transduction pathways." Proceedings of the National Academy of Sciences **97**(12): 6499-6503.
Clurman, B. E. and J. M. Roberts (1995). "Cell Cycle and Cancer." J. Natl. Cancer Inst. **87**(20): 1499-1501.
Cormack, B. P., R. H. Valdivia, et al. (1996). "FACS-optimized mutants of the green fluorescent protein (GFP)." Gene **173**(1): 33-38.
Davis, C. G., J. L. Goldstein, et al. (1987). "Acid-dependent ligand dissociation and recycling of LDL receptor mediated by growth factor homology region." Nature **326**(6115): 760-5.
Dawson, W. O., D. L. Beck, et al. (1986). "cDNA cloning of the complete genome of tobacco mosaic virus and production of infectious transcripts." Proc Natl Acad Sci U S A **83**(6): 1832-1836.
de Duve, C. (1963). Lysosomes. Ciba Foundation Symposium. A. V. S. de Reuck and M. P. Cameron. London, Churchill**:** 411-2.
Dean, P. N. and J. H. Jett (1974). "Mathematical analysis of DNA distributions derived from flow microfluorometry." J Cell Biol **60**(2): 523-7.
Derossi, D., S. Calvet, et al. (1996). "Cell Internalization of the Third Helix of the Antennapedia Homeodomain Is Receptor-independent
10.1074/jbc.271.30.18188." J. Biol. Chem. **271**(30): 18188-18193.
Derossi, D., A. H. Joliot, et al. (1994). "The third helix of the Antennapedia homeodomain translocates through biological membranes." J Biol Chem **269**(14): 10444-50.
Dhillon, N. K. and M. Mudryj (2003). "Cyclin E overexpression enhances cytokine-mediated apoptosis in MCF7 breast cancer cells." Genes and Immunity **4**(5): 336-342.
Ding, X. S., J. Z. Liu, et al. (2004). "The Tobacco mosaic virus 126-kDa protein associated with virus replication and movement suppresses RNA silencing." Molecular Plant-Microbe Interactions **17**(6): 583-592.

Drygin, Y. F., O. A. Bordunova, et al. (1998). "Atomic force microscopy examination of tobacco mosaic virus and virion RNA." FEBS Letters **425**(2): 217-221.
Dubrovsky, J. G. and V. B. Ivanov (2003). "Celebrating 50 years of the cell cycle." **426**(6968): 759.
Durham, A. C. (1978). "The roles of small ions, especially calcium, in virus disassembly, takeover, and transformation." Biomedicine **28**(6): 307-13.
Durham, A. C. H. (1972). "Structures and Roles of Polymorphic Forms of Tobacco Mosaic Virus Protein .1. Sedimentation Studies." Journal of Molecular Biology **67**(2): 289-306.
Durham, A. C. H., J. T. Finch, et al. (1971). "States of Aggregation of Tobacco Mosaic Virus Protein." Nature-New Biology **229**(2): 37-&.
Durham, A. C. H., D. A. Hendry, et al. (1977). "Does Calcium-Ion Binding Control Plant-Virus Disassembly." Virology **77**(2): 524-533.
Ekholm, S. V., P. Zickert, et al. (2001). "Accumulation of cyclin E is not a prerequisite for passage through the restriction point." Molecular and Cellular Biology **21**(9): 3256-3265.
Elbashir, S. M., J. Harborth, et al. (2001). "Duplexes of 21-nucleotide RNAs mediate RNA interference in cultured mammalian cells." Nature **411**(6836): 494-8.
Elliott, G. and P. O'Hare (1997). "Intercellular trafficking and protein delivery by a herpesvirus structural protein." Cell **88**(2): 223-33.
Fire, A., S. Xu, et al. (1998). "Potent and specific genetic interference by double-stranded RNA in caenorhabditis elegans." Nature **391**(6669): 806-811.
Fox, M. H. (1980). "A model for the computer analysis of synchronous DNA distributions obtained by flow cytometry." Cytometry **1**(1): 71-7.
Fraenkel-Conrat, H. (1957). "Degradation of Tobacco Mosaic Virus with Acetic Acid." Virology **4**(1): 1-4.
Fraenkel-Conrat, H. and R. C. Williams (1955). "Reconstitution of Active Tobacco Mosaic Virus from Its Inactive Protein and Nucleic Acid Components." PNAS **41**(10): 690-698.
Frankel, A. D. and C. O. Pabo (1988). "Cellular uptake of the tat protein from human immunodeficiency virus." Cell **55**(6): 1189-1193.
Funk, J. O. (2005). Cell cycle checkpoint genes and cancer. Encyclopedia of Life Sciences, John Wiley & Sons, Ltd.
Gaddipati, J. P., C. D. Atreya, et al. (1988). "Characterization of the Tmv Encapsidation Initiation Site on 18s Ribosomal-Rna." Nucleic Acids Research **16**(15): 7303-7313.
Gaddipati, J. P. and A. Siegel (1990). "Study of TMV assembly with heterologous RNA containing the origin-of-assembly sequence." Virology **174**(2): 337-44.
Gallie, D. R., D. E. Sleat, et al. (1987). "The 5'-Leader Sequence of Tobacco Mosaic-Virus Rna Enhances the Expression of Foreign Gene Transcripts Invitro and Invivo." Nucleic Acids Research **15**(8): 3257-3273.
Gallie, D. R., D. E. Sleat, et al. (1988). "Mutational Analysis of the Tobacco Mosaic-Virus 5'-Leader for Altered Ability to Enhance Translation." Nucleic Acids Research **16**(3): 883-893.
Gilmore, I. R., S. P. Fox, et al. (2006). "Delivery Strategies for siRNA-mediated Gene Silencing." Current Drug Delivery **3**(2): 147-155.

Goelet, P., G. P. Lomonossoff, et al. (1982). "Nucleotide-Sequence of Tobacco Mosaic-Virus Rna." Proceedings of the National Academy of Sciences of the United States of America-Biological Sciences **79**(19): 5818-5822.
Goldstein, J. L., M. S. Brown, et al. (1985). "Receptor-mediated endocytosis: concepts emerging from the LDL receptor system." Annu Rev Cell Biol **1**: 1-39.
Gooding, G. V. and T. T. Hebert (1967). "A Simple Technique for Purification of Tobacco Mosaic Virus in Large Quantities." Phytopathology **57**(11): 1285-&.
Grassi, G., A. Schneider, et al. (2005). "Hammerhead ribozymes targeted against cyclin E and E2F1 cooperate to down-regulate coronary smooth muscle cell proliferation." Journal of Gene Medicine **7**(9): 1223-1234.
Green, M. and P. M. Loewenstein (1988). "Autonomous functional domains of chemically synthesized human immunodeficiency virus tat trans-activator protein." Cell **55**(6): 1179-1188.
Greenberg, S. and S. C. Silverstein (1993). Phagocytosis. Fundamental Immunology. W. E. Paul. New York, Faven**:** 941-64.
Griffin, F. M., Jr., J. A. Griffin, et al. (1975). "Studies on the mechanism of phagocytosis. I. Requirements for circumferential attachment of particle-bound ligands to specific receptors on the macrophage plasma membrane." J Exp Med **142**(5): 1263-82.
Griffin, F. M., Jr., J. A. Griffin, et al. (1976). "Studies on the mechanism of phagocytosis. II. The interaction of macrophages with anti-immunoglobulin IgG-coated bone marrow-derived lymphocytes." J Exp Med **144**(3): 788-809.
Guo, S. and K. J. Kemphues (1995). "par-1, a gene required for establishing polarity in C. elegans embryos, encodes a putative Ser/Thr kinase that is asymmetrically distributed." Cell **81**(4): 611-20.
Gurzov, E. N. and M. Izquierdo (2006). "Cyclin E1 knockdown induces apoptosis in cancer cells." Neurol Res **28**(5): 493-9.
Haas, J., E. C. Park, et al. (1996). "Codon usage limitation in the expression of HIV-1 envelope glycoprotein." Current Biology **6**(3): 315-324.
Hall, A. H., J. Wan, et al. (2004). "RNA interference using boranophosphate siRNAs: structure-activity relationships." Nucleic Acids Res **32**(20): 5991-6000.
Hall, A. H., J. Wan, et al. (2006). "High potency silencing by single-stranded boranophosphate siRNA." Nucleic Acids Res **34**(9): 2773-81.
Hannon, G. J. (2002). "RNA interference." Nature **418**(6894): 244-251.
Harrison, B. D. and T. M. A. Wilson (1999). "Milestones in the research on tobacco mosaic virus." Philosophical Transactions of the Royal Society of London Series B-Biological Sciences **354**(1383): 521-529.
Hogrefe, R. I., A. V. Lebedev, et al. (2006). "Chemically modified short interfering hybrids (siHYBRIDS): nanoimmunoliposome delivery in vitro and in vivo for RNAi of HER-2." Nucleosides Nucleotides Nucleic Acids **25**(8): 889-907.
Holen, T., M. Amarzguioui, et al. (2003). "Similar behaviour of single-strand and double-strand siRNAs suggests they act through a common RNAi pathway." Nucleic Acids Res **31**(9): 2401-7.
Hwang, H. C. and B. E. Clurman (2005). "Cyclin E in normal and neoplastic cell cycles." Oncogene **24**(17): 2776-2786.

Ivanowski, D. (1892). "Ueber die Mosaikkrankheit der Tabakspflanze." St. Petersb. Acad. Imp. Sci. Bull. **35**: 65-70.
Jia, F., Y. Z. Zhang, et al. (2006). "A retrovirus-based system to stably silence hepatitis B virus genes by RNA interference." Biotechnology Letters **28**(20): 1679-1685.
Jing, S. Q., T. Spencer, et al. (1990). "Role of the human transferrin receptor cytoplasmic domain in endocytosis: localization of a specific signal sequence for internalization." J Cell Biol **110**(2): 283-94.
Joensuu, J., V. Niklander-Teeri, et al. (2008). "Transgenic plants for animal health: plant-made vaccine antigens for animal infectious disease control." Phytochemistry Reviews.
Joliot, A., C. Pernelle, et al. (1991). "Antennapedia Homeobox Peptide Regulates Neural Morphogenesis." Proceedings of the National Academy of Sciences **88**(5): 1864-1868.
Jonard, G., K. E. Richards, et al. (1977). "Sequence from Assembly Nucleation Region of Tmv Rna." Cell **11**(3): 483-493.
Jones, S. W., R. Christison, et al. (2005). "Characterisation of cell-penetrating peptide-mediated peptide delivery." Br J Pharmacol **145**(8): 1093-102.
Kado, C. I. and C. A. Knight (1966). "Location of a Local Lesion Gene in Tobacco Mosaic Virus RNA." Proceedings of the National Academy of Sciences of the United States of America **55**(5): 1276-1283.
Kaiser, J. (2007). "GENE THERAPY: Questions Remain on Cause of Death in Arthritis Trial." Science **317**(5845): 1665a-.
Kalluri, R. and K. Kanasaki (2008). "RNA interference: Generic block on angiogenesis." Nature **452**(7187): 543-545.
Kanaseki, T. and K. Kadota (1969). "The "vesicle in a basket". A morphological study of the coated vesicle isolated from the nerve endings of the guinea pig brain, with special reference to the mechanism of membrane movements." J Cell Biol **42**(1): 202-20.
Kang, J., H. G. Lemaire, et al. (1987). "The precursor of Alzheimer's disease amyloid A4 protein resembles a cell-surface receptor." Nature **325**(6106): 733-6.
King, L. and R. N. Perham (1971). "Reaction of Tobacco Mosaic Virus with Maleic Anhydride and Some Possible Applications to X-Ray Diffraction Analysis." Biochemistry **10**(6): 981-&.
Kleinman, M. E., K. Yamada, et al. (2008). "Sequence- and target-independent angiogenesis suppression by siRNA via TLR3." **452**(7187): 591-597.
Klug, A. (1999). "The tobacco mosaic virus particle: structure and assembly." Philosophical Transactions of the Royal Society of London Series B-Biological Sciences **354**(1383): 531-535.
Koff, A., F. Cross, et al. (1991). "Human Cyclin-E, a New Cyclin That Interacts with 2 Members of the Cdc2 Gene Family." Cell **66**(6): 1217-1228.
Koo, E. H. and S. L. Squazzo (1994). "Evidence that production and release of amyloid beta-protein involves the endocytic pathway." J Biol Chem **269**(26): 17386-9.
Lawrencia, C., R. Mahendran, et al. (2001). "Transfection of urothelial cells using methyl-beta-cyclodextrin solubilized cholesterol and Dotap." Gene Ther **8**(10): 760-8.

Lee, S. Y., E. Royston, et al. (2005). "Improved metal cluster deposition on a genetically engineered tobacco mosaic virus template." Nanotechnology **16**(7): S435-S441.
Lewandowski, D. J. and W. O. Dawson (2000). "Functions of the 126- and 183-kDa Proteins of Tobacco Mosaic Virus." Virology **271**(1): 90-98.
Lewin, M., N. Carlesso, et al. (2000). "Tat peptide-derivatized magnetic nanoparticles allow in vivo tracking and recovery of progenitor cells." Nature Biotechnology **18**(4): 410-414.
Lin, L., L. X. Chen, et al. (2006). "Adenovirus-mediated transfer of siRNA against Runx2/Cbfa1 inhibits the formation of heterotopic ossification in animal model." Biochemical and Biophysical Research Communications **349**(2): 564-572.
Liu, G., F. Wong-Staal, et al. (2007). "Development of new RNAi therapeutics." Histology and Histopathology **22**(2): 211-217.
Lobel, P., K. Fujimoto, et al. (1989). "Mutations in the cytoplasmic domain of the 275 kd mannose 6-phosphate receptor differentially alter lysosomal enzyme sorting and endocytosis." Cell **57**(5): 787-96.
Lu, B., G. Stubbs, et al. (1996). "Carboxylate interactions involved in the disassembly of tobacco mosaic tobamovirus." Virology **225**(1): 11-20.
Lu, B., Z. F. Taraporewala, et al. (1998). "Intersubunit interactions allowing a carboxylate mutant coat protein to inhibit tobamovirus disassembly." Virology **244**(1): 13-19.
March, J. C. and W. E. Bentley (2007). "RNAi-based tuning of cell cycling in Drosophila S2 cells - effects on recombinant protein yield." Applied Microbiology and Biotechnology **73**(5): 1128-1135.
Marques, J. T. and B. R. Williams (2005). "Activation of the mammalian immune system by siRNAs." Nat Biotechnol **23**(11): 1399-405.
Martinez, J., A. Patkaniowska, et al. (2002). "Single-stranded antisense siRNAs guide target RNA cleavage in RNAi." Cell **110**(5): 563-74.
Matzke, M. A. (2002). "Gene silencing mechanisms illuminate new pathways of disease resistance." Transgenic Res **11**(6): 637-8.
McGraw, T. E. and F. R. Maxfield (1990). "Human transferrin receptor internalization is partially dependent upon an aromatic amino acid on the cytoplasmic domain." Cell Regul **1**(4): 369-77.
Meister, G. and T. Tuschl (2004). "Mechanisms of gene silencing by double-stranded RNA." Nature **431**(7006): 343-9.
Meshi, T., T. Ohno, et al. (1981). "Nucleotide-Sequence of a Cloned Cdna Copy of Tmv (Cowpea Strain) Rna, Including the Assembly Origin, the Coat Protein Cistron, and the 3' Non-Coding Region." Molecular & General Genetics **184**(1): 20-25.
Metchnikoff, E. (1893). Lectures on the Comparative Pathology of Imflammation.
Miettinen, H. M., J. K. Rose, et al. (1989). "Fc receptor isoforms exhibit distinct abilities for coated pit localization as a result of cytoplasmic domain heterogeneity." Cell **58**(2): 317-27.
Morimoto, H., H. Okamura, et al. (2004). "Double-stranded RNA mediates selective gene silencing of protein phosphatase type 1 delta isoform in HEK-293 cells." J Enzyme Inhib Med Chem **19**(4): 327-31.

Muller, W. A., R. M. Steinman, et al. (1980). "The membrane proteins of the vacuolar system. II. Bidirectional flow between secondary lysosomes and plasma membrane." J Cell Biol **86**(1): 304-14.
Muller, W. A., R. M. Steinman, et al. (1983). "Membrane proteins of the vacuolar system. III. Further studies on the composition and recycling of endocytic vacuole membrane in cultured macrophages." J Cell Biol **96**(1): 29-36.
Mundry, K. W., P. A. C. Watkins, et al. (1991). "Complete Uncoating of the 5' Leader Sequence of Tobacco Mosaic-Virus Rna Occurs Rapidly and Is Required to Initiate Cotranslational Virus Disassembly Invitro." Journal of General Virology **72**: 769-777.
Nakahara, K. and R. W. Carthew (2004). "Expanding roles for miRNAs and siRNAs in cell regulation." Current Opinion in Cell Biology **16**(2): 127-133.
Namba, K., R. Pattanayek, et al. (1989). "Visualization of protein-nucleic acid interactions in a virus. Refined structure of intact tobacco mosaic virus at 2.9 A resolution by X-ray fiber diffraction." J Mol Biol **208**(2): 307-25.
Nicolaie, A., G. Lebeurie, et al. (1974). "Electron-Microscopy and Infectivity Studies of Action of Dimethylsulfoxide on 2 Strains of Tobacco Mosaic-Virus." Journal of General Virology **22**(JAN): 43-53.
Nordstedt, C., G. L. Caporaso, et al. (1993). "Identification of the Alzheimer beta/A4 amyloid precursor protein in clathrin-coated vesicles purified from PC12 cells." J Biol Chem **268**(1): 608-12.
Novak, B., J. Sible, et al. (2003). Checkpoints in cell cycle. Encyclopedia of Life Sciences, John Wiley & Sons, Ltd.
Nykanen, A., B. Haley, et al. (2001). "ATP requirements and small interfering RNA structure in the RNA interference pathway." Cell **107**(3): 309-321.
Okada, Y. (1986). "Molecular assembly of tobacco mosaic virus in vitro." Advances in Biophysics **22**: 95-149.
Okada, Y., M. Fukuda, et al. (1980). "Initiation Site for Assembly of Several Strains of Tmv and Its Relation to Occurrence of the Short Particles in Infected Plants." Biosystems **12**(3-4): 257-264.
Omidi, Y., A. J. Hollins, et al. (2005). "Polypropylenimine dendrimer-induced gene expression changes: the effect of complexation with DNA, dendrimer generation and cell type." J Drug Target **13**(7): 431-43.
Pelham, H. R. B. (1978). "Leaky Uag Termination Codon in Tobacco Mosaic-Virus Rna." Nature **272**(5652): 469-471.
Phelan, A., G. Elliott, et al. (1998). "Intercellular delivery of functional p53 by the herpesvirus protein VP22." Nat Biotechnol **16**(5): 440-3.
Pooga, M., C. Kut, et al. (2001). "Cellular translocation of proteins by transportan." Faseb J **15**(8): 1451-3.
Porter, P. L., K. E. Malone, et al. (1997). "Expression of cell-cycle regulators p27(Kip1) and cyclin E, alone and in combination, correlate with survival in young breast cancer patients." Nature Medicine **3**(2): 222-225.
Predescu, D., R. Horvat, et al. (1994). "Transcytosis in the continuous endothelium of the myocardial microvasculature is inhibited by N-ethylmaleimide." Proc Natl Acad Sci U S A **91**(8): 3014-8.

Rabinovitch, P. S. (1994). "DNA content histogram and cell-cycle analysis." Methods Cell Biol **41**: 263-96.
Raemdonck, K., K. Remaut, et al. (2006). "In situ analysis of single-stranded and duplex siRNA integrity in living cells." Biochemistry **45**(35): 10614-10623.
Rossi, J. J. (2004). "Medicine: a cholesterol connection in RNAi." Nature **432**(7014): 155-6.
Rossi, J. J. (2005). "Receptor-targeted siRNAs." Nat Biotechnol **23**(6): 682-4.
Roth, T. F. and K. R. Porter (1964). "Yolk Protein Uptake in the Oocyte of the Mosquito Aedes Aegypti. L." J Cell Biol **20**: 313-32.
Rothbard, J. B., S. Garlington, et al. (2000). "Conjugation of arginine oligomers to cyclosporin A facilitates topical delivery and inhibition of inflammation." Nat Med **6**(11): 1253-7.
Saydam, O., D. L. Glauser, et al. (2005). "Herpes simplex virus 1 amplicon vector-mediated siRNA targeting epidermal growth factor receptor inhibits growth of human glioma cells in vivo." Molecular Therapy **12**(5): 803-812.
Schagen, F. H., H. J. Rademaker, et al. (2000). "Insertion vectors for gene therapy." Gene Ther **7**(4): 271-2.
Schwarz, D. S., G. Hutvagner, et al. (2002). "Evidence that siRNAs function as guides, not primers, in the Drosophila and human RNAi pathways." Molecular Cell **10**(3): 537-548.
Schwarze, S. R., A. Ho, et al. (1999). "In Vivo Protein Transduction: Delivery of a Biologically Active Protein into the Mouse." Science **285**(5433): 1569.
Shaw, J. G., K. A. Plaskitt, et al. (1986). "Evidence That Tobacco Mosaic-Virus Particles Disassemble Cotranslationally In vivo." Virology **148**(2): 326-336.
Shyng, S. L., J. E. Heuser, et al. (1994). "A glycolipid-anchored prion protein is endocytosed via clathrin-coated pits." J Cell Biol **125**(6): 1239-50.
Shyng, S. L., K. L. Moulder, et al. (1995). "The N-terminal domain of a glycolipid-anchored prion protein is essential for its endocytosis via clathrin-coated pits." J Biol Chem **270**(24): 14793-800.
Silber, G. and L. G. Burk (1965). "Infectivity of Tobacco Mosaic Virus Stored for 50 Years in Extracted Unpreserved Plant Juice." Nature **206**(4985): 740-&.
Sioud, M. (2006). "RNAi therapy: antibodies guide the way." Gene Ther **13**(3): 194-5.
Sioud, M. and D. R. Sorensen (2003). "Cationic liposome-mediated delivery of siRNAs in adult mice." Biochemical and Biophysical Research Communications **312**(4): 1220-1225.
Sleat, D. E., D. R. Gallie, et al. (1987). "Characterization of the 5'-Leader Sequence of Tobacco Mosaic-Virus Rna as a General Enhancer of Translation Invitro." Gene **60**(2-3): 217-225.
Sorensen, D. R., M. Leirdal, et al. (2003). "Gene silencing by systemic delivery of synthetic siRNAs in adult mice." Journal of Molecular Biology **327**(4): 761-766.
Staczek, J., M. Bendahmane, et al. (2000). "Immunization with a chimeric tobacco mosaic virus containing an epitope of outer membrane protein F of Pseudomonas aeruginosa provides protection against challenge with P. aeruginosa." Vaccine **18**(21): 2266-2274.

Steckert, J. J. and T. M. Schuster (1982). "Sequence specificity of trinucleoside diphosphate binding to polymerized tobacco mosaic virus protein." Nature **299**(5878): 32-6.
Stubbs, G. (1990). "Molecular structures of viruses from the tobacco mosaic virus group." Seminars in Virology **1**: 405-12.
Sutherland, R. and E. Musgrove (2002). "Cyclin D1 and mammary carcinoma: new insights from transgenic mouse models." Breast Cancer Res **4**(1): 14 - 17.
Swanson, J. A. and S. C. Baer (1995). "Phagocytosis by zippers and triggers." Trends Cell Biol **5**(3): 89-93.
Tabas, I. (1995). "The stimulation of the cholesterol esterification pathway by atherogenic lipoproteins in macrophages." Curr Opin Lipidol **6**(5): 260-8.
Tang, G. (2005). "siRNA and miRNA: an insight into RISCs." Trends Biochem Sci **30**(2): 106-14.
Tkachenko, A. G., H. Xie, et al. (2003). "Multifunctional gold nanoparticle-peptide complexes for nuclear targeting." Journal of the American Chemical Society **125**(16): 4700-4701.
Turner, D. R. and P. J. G. Butler (1986). "Essential Features of the Assembly Origin of Tobacco Mosaic-Virus Rna as Studied by Directed Mutagenesis." Nucleic Acids Research **14**(23): 9229-9242.
Turner, D. R., L. E. Joyce, et al. (1988). "The Tobacco Mosaic-Virus Assembly Origin Rna - Functional-Characteristics Defined by Directed Mutagenesis." Journal of Molecular Biology **203**(3): 531-547.
Turpen, T. H., S. J. Reinl, et al. (1995). "Malarial Epitopes Expressed on the Surface of Recombinant Tobacco Mosaic-Virus." Bio-Technology **13**(1): 53-57.
Turpen, T. H., A. M. Turpen, et al. (1993). "Transfection of Whole Plants from Wounds Inoculated with Agrobacterium-Tumefaciens Containing Cdna of Tobacco Mosaic-Virus." Journal of Virological Methods **42**(2-3): 227-240.
Tyc, K., M. Konarska, et al. (1984). "Multiple ribosome binding to the 5'-terminal leader sequence of tobacco mosaic virus RNA. Assembly of an 80S ribosome -mRNA complex at the AUU codon." European Journal of Biochemistry **140**(3): 503-511.
van den Heuvel, S. (2005). "Cell-cycle regulation." WormBook: 1-16.
Vermij, P. (2006). "USDA approves the first plant-based vaccine." Nature Biotechnology **24**(3): 234.
Vives, E., P. Brodin, et al. (1997). "A truncated HIV-1 Tat protein basic domain rapidly translocates through the plasma membrane and accumulates in the cell nucleus." J Biol Chem **272**(25): 16010-7.
Wender, P. A., D. J. Mitchell, et al. (2000). "The design, synthesis, and evaluation of molecules that enable or enhance cellular uptake: peptoid molecular transporters." Proc Natl Acad Sci U S A **97**(24): 13003-8.
Wianny, F. and M. Zernicka-Goetz (2000). "Specific interference with gene function by double-stranded RNA in early mouse development." Nat Cell Biol **2**(2): 70-5.
Wilson, T. M., R. N. Perham, et al. (1976). "Polarity of the RNA in the tobacco mosaic virus particle and the direction of protein stripping in sodium dodecyl sulphate." FEBS Lett **64**(2): 285-9.
Wilson, T. M. A. (1984). "Cotranslational Disassembly of Tobacco Mosaic-Virus Invitro." Virology **137**(2): 255-265.

Wilson, T. M. A. and J. G. Shaw (1986). "Cotranslational Disassembly of Plant-Virus Nucleocapsids." Journal of Cellular Biochemistry: 271-271.
Yang, S., S. Tutton, et al. (2001). "Specific double-stranded RNA interference in undifferentiated mouse embryonic stem cells." Mol Cell Biol **21**(22): 7807-16.
Yang, T. T., L. Z. Cheng, et al. (1996). "Optimized codon usage and chromophore mutations provide enhanced sensitivity with the green fluorescent protein." Nucleic Acids Research **24**(22): 4592-4593.
Yi, H. M., S. Nisar, et al. (2005). "Patterned assembly of genetically modified viral nanotemplates via nucleic acid hybridization." Nano Letters **5**(10): 1931-1936.
Zeng, Y., R. Yi, et al. (2003). "MicroRNAs and small interfering RNAs can inhibit mRNA expression by similar mechanisms." Proceedings of the National Academy of Sciences **100**(17): 9779-9784.
Zeyenko, V. V., L. A. Ryabova, et al. (1994). "Enhancing effect of the 3'-untranslated region of tobacco mosaic virus RNA on protein synthesis in vitro." FEBS Letters **354**(3): 271-273.
Zhang, F., P. Andreassen, et al. (1999). "A transfecting peptide derived from adenovirus fiber protein." Gene Ther **6**(2): 171-81.
Zimmern, D. and P. J. G. Butler (1977). "Isolation of Tobacco Mosaic-Virus Rna Fragments Containing Origin for Viral Assembly." Cell **11**(3): 455-462.